Spectrally Efficient Uplink Cooperative NOMA With Joint Decoding for Relay-Assisted IoT Networks

Jeong Seon Yeom, *Student Member, IEEE*, Young-Bin Kim, *Member, IEEE*, and Bang Chul Jung, *Senior Member, IEEE*

***Abstract*—We propose a spectrally efficient uplink cooperative relaying protocol with K multiple half-duplex relay stations (RNs) for wireless Internet of Things (IoT) networks, where two IoT devices (IDs) and an access point (AP) cannot directly communicate with each other. The two IDs simultaneously transmit signals over the same spectrum resource using the nonorthogonal multiple access (NOMA) technique. In the proposed technique, at a certain time slot, a single RN is selected to send the received packets from two IDs in the previous time slot, while the remaining $K-1$ RNs receive new packets from two IDs. Thus, the proposed relaying protocol can send N packets from an ID to the AP during $N+1$ time slots without a duty-cycle loss in conventional half-duplex relaying schemes. We call the proposed protocol a *spectrally efficient* cooperative NOMA. The main highlight of our results is that we mathematically derive a closed-form outage probability of the proposed protocol by considering inter-relay interference, assuming an optimal joint decoding technique instead of successive interference cancelation (SIC) decoding at each RN. To the best of our knowledge, this is the first theoretical result in the literature. Extensive computer simulations are used to validate the mathematical results. Furthermore, it is shown that the proposed protocol significantly outperforms the existing two-hop half-duplex cooperative NOMA technique and the SIC decoding scheme in terms of outage probability.**

***Index Terms*—Cooperative relaying protocol, Internet of Things (IoT) networks, joint decoding (JD), nonorthogonal multiple access (NOMA), outage probability, spectral efficiency.**

I. Introduction

MASSIVE Internet of Things (IoT) networks comprising enormous devices, such as vehicles, sensors, and wearable devices have been attracting significant attention not only in fifth-generation (5G) wireless communication systems but also in sixth-generation (6G) wireless communication systems. In massive IoT networks, energy efficiency, short data transmission, energy harvesting, access barring protocols, and random access are essential issues to be considered [1], [2]. In 6G, in particular, the ultramassive machine-type communication scenario is expected to require a connection density of $10^6/\text{km}^2$, which is ten times the connection density of 5G [3]. More radio resources (typically spectral resources) are required as the number of wireless devices increases. One of the most challenging issues for future wireless IoT networks is to enhance spectral efficiency further to accommodate the exponentially increasing number of devices. Hence, spectrally efficient technologies have been studied extensively, from signal modulation to network design for massive IoT networks [4], [5], [6], [7], [8].

Nonorthogonal multiple access (NOMA) techniques have attracted significant attention both from academia and industry as promising solutions for improving the spectral efficiency, which results in higher sum-rate and sum-throughput than those in the conventional orthogonal multiple access (OMA) techniques [9], [10]. NOMA techniques are generally classified into power domain (PD)-NOMA and code domain (CD)-NOMA techniques. In particular, PD-NOMA was actively studied as a study item in 3GPP LTE Release 13, and it has been widely investigated due to its precise theoretical analysis and outstanding performance [11].

The NOMA technique has been applied to relay-based wireless IoT networks to improve energy efficiency which is one of the vital requirements for battery-powered IoT devices (IDs) [12]. Many relay-aided NOMA systems with a *single* relay node (RN) have been investigated in various communication scenarios [13], [14], [15], [16], [17], [18], [19], [20], [21]. In [14], a downlink cooperative NOMA system with half-duplex and amplify-forward (AF) RNs was approximately analyzed in terms of the outage probability, where only one user, e.g., a cell-edge user (CEU), is supported by the RN because of the absence of a direct link between a base station (BS) and the user. A downlink cooperative NOMA system was also investigated in the presence of a direct link between the BS and users [17]. In this study, two cooperative relaying schemes are proposed for the BS-to-user link and the RN-to-user link based on decoding conditions to reduce error propagation caused by successive interference cancellation (SIC) decoding and avoid unnecessary relaying

Manuscript received 12 April 2022; revised 14 July 2022; accepted 11 August 2022. Date of publication 26 August 2022; date of current version 22 December 2022. This work was supported in part by the National Research Foundation of Korea (NRF) through Basic Research Laboratory (BRL) Program funded by the Korea Government (MSIT) under Grant NRF-2021R1A4A1032580, and in part by the Institute for Information and communications Technology Promotion (IITP) through Augmented Beam-routing: Carom-MIMO funded by the Korea Government (MSIT) under Grant 2021-0-00486. *(Corresponding author: Bang Chul Jung.)*

Jeong Seon Yeom and Bang Chul Jung are with the Department of Electronics Engineering, Chungnam National University, Daejeon 34134, Republic of Korea (e-mail: jsyeom@cnu.ac.kr; bcjung@cnu.ac.kr).

Young-Bin Kim was with the Future Access Network Division, KDDI Research, Inc., Saitama 356-8502, Japan. He is now the Field Application Engineer, VIAVI Solutions Japan, Inc., Tokyo 163-1107, Japan (e-mail: youngbin.kim@viavisolutions.com).

Digital Object Identifier 10.1109/JIOT.2022.3202006

transmission, respectively. For an uplink cooperative NOMA system, a half-duplex and decode–forward (DF) RN was considered [15], [18]. In particular, the ergodic capacity was analyzed under interference at the RN due to imperfect SIC operations [15], and the outage probability was analyzed under the assumption of Nakagami-*m* fading channels [18]. In [21], a downlink NOMA technique in full-duplex two-hop systems was considered with in-phase and quadrature imbalance and imperfect SIC, where the authors mathematically analyzed the outage probability and ergodic sum-rate performances. To improve the spectral efficiency, a full-duplex RN with multiple transmit/receive antennas was applied to cooperative NOMA systems, where transmit/receive zero-forcing beamforming techniques and maximum-ratio transmission/combining were exploited [19].

However, the full-duplex relaying protocol may reduce the signal-to-interference-plus-noise ratio (SINR) at the RN, owing to residual self-interference. It is not easy to guarantee that the self-interference of the full-duplex RN is perfectly removed. The level of self-interference can be in the order of 60–100 dB stronger than the desired signal of interest at the receiver input, as reported in [22]. Furthermore, the residual self-interference due to channel estimation or quantization error may induce significant performance degradation [19], [23], [24].

Relay-aided NOMA systems with a single RN have been extended to cooperative NOMA systems that exploit multiple RNs to improve diversity gain. In [25], multiple RNs were used to send the received signal from the BS to one user group, where a joint power allocation and transmission scheduling algorithm was proposed to maximize the overall system throughput. However, the simultaneous transmission of multiple RNs in two-hop relaying networks induces significant signaling overhead, e.g., power allocation and channel state information in general. In [26], an RN selection scheme was proposed in a full-duplex AF RN-aided downlink NOMA system. In order to improve the SINR at the destination, only a single RN with the maximum SINR in the first hop is selected to transmit the downlink NOMA signal to two devices. The best single RN selection technique was proposed in a two-hop NOMA system [27], where the RN with the strongest channel gain to the CEU among RNs that succeeds in decoding is selected for relaying the packet. For downlink NOMA systems, a two-stage max-min RN selection scheme and a two-stage DF/AF RN selection based on adaptive power allocation have been proposed [28], [29], respectively. In addition, combined RN selection and adaptive power allocation schemes were proposed for downlink cooperative NOMA systems, and their outage probability and diversity gain were analyzed [30]. The impact of RN selection on the performance of the downlink cooperative NOMA system was investigated, where each RN was assumed to operate in a full-duplex or half-duplex mode [31]. In particular, imperfect self-interference cancelation at the full-duplex RN was considered, and the outage probability was mathematically analyzed in [31]. Recently, a novel spectrally efficient cooperative relaying protocol was proposed for a downlink NOMA system, where the proposed technique compensates for the multiplexing loss due to the half-duplex operation of multiple RNs via successive relaying operation [32], [33]. The selected RN sends packets to two downlink users at the second hop, whereas the BS sends new packets to other RNs, except for the selected RN, simultaneously [32], [33]. Thus, the spectral efficiency is approximately similar to that of full-duplex RN-based cooperative NOMA [33].

In summary, existing studies on cooperative NOMA with multiple RNs in the literature have considered *downlink* networks even though the amount of uplink traffic tends to be larger than the amount of downlink traffic for practical massive IoT networks [34]. Thus, it is essential to improve the spectral efficiency of the uplink rather than the downlink, considering IoT applications. NOMA techniques are being actively investigated for efficiently supporting a large number of IDs [34]. Battery-powered IDs are required to operate with low power consumption in practice, which results in limited coverage. Thus, a relay-assisted IoT (R-IoT) network needs to be considered, especially for uplink [12].

To address the above-mentioned issues, in this article, we propose a novel spectrally efficient uplink cooperative NOMA protocol for R-IoT networks comprising two IDs, multiple half-duplex DF RNs, and a single access point (AP) equipped with multiple antennas. As a main result, we mathematically analyze the exact outage probability of the proposed cooperative NOMA protocol with a joint decoding (JD) technique at each RN, which has not been discussed in the existing literature, including [32], [33]. Our derived *closed-form* mathematical expressions for performance metrics enable for us to exactly estimate the performance, such as outage probability and effective throughput in various system parameters, which can help a system designer to optimize the network with a computationally efficient manner. It is worth noting that the JD achieves the optimal decoding performance in terms of throughput and error probability [35], [36]. The condition for successful decoding of the JD technique is determined based on the boundary of the *m*-user multiple access channel (MAC) capacity region, which is the closure of the convex hull of the rate vectors, $R(S)$, satisfying

$$R(S) \leq I\big(X(S); Y \mid X\big(S^c\big)\big) \quad \forall S \subseteq \{1, 2, \ldots m\} \tag{1}$$

where $Y = \sum_{i\in\{1,2,\ldots m\}} H_i X_i + Z$ for fading channels. Please refer to [35, Ch. 15.3.5] for the detailed description of the variables in (1). The case where the boundary condition of the MAC capacity is satisfied for all subsets S in (1) is defined as the decoding success condition of the JD. The JD technique is the optimal in terms of both achievable rate and outage probability.

The performance enhancement by exploiting the JD instead of the SIC decoding in terms of the outage probability and sum-throughput has been verified in uplink NOMA systems [37], [38], [39]. In addition, the fairness among users is one of the important performance metrics in NOMA-based systems. In particular, if we consider the SIC scheme in the receiver of NOMA systems, then the decoding order significantly affects the achievable rate of users and the fairness among users. The fairness problem in the SIC-based *downlink* NOMA system may be solved through adaptive power

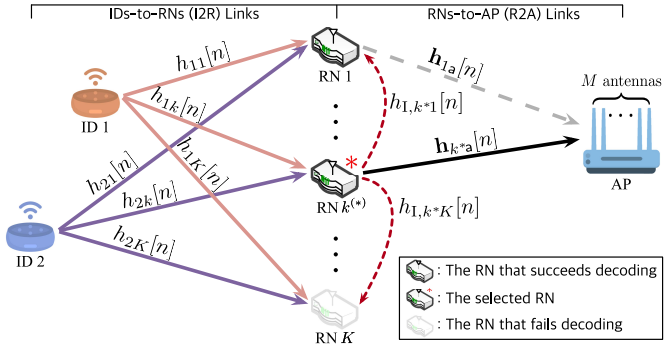

Fig. 1. Uplink cooperative NOMA system with multiple RNs.

allocation and decoding order control [40]. However, this technique requires a delicate control from the AP to IDs based on instantaneous channel state information, which seems not to be feasible in relay-assisted massive IoT networks. It is worth noting that the JD technique can provide the optimal fairness among IDs for uplink NOMA systems since it achieves all rate pairs of multiple IDs. Furthermore, extensive computer simulations show that the proposed protocol outperforms the existing two-hop relaying protocol and the SIC scheme in terms of outage probability and effective throughput.

The remainder of this article is organized as follows. In Section II, we describe the system model, and we explain the proposed spectrally efficient cooperative NOMA protocol as well as the existing two-hop half-duplex uplink NOMA protocol. The proposed technique is mathematically analyzed in terms of the outage probability and the diversity order in Section III. The numerical results are presented in Section IV, and conclusions are drawn in Section V.

II. System Model and Proposed Spectrally Efficient Cooperative NOMA Protocol

In this section, we describe an uplink NOMA system with multiple cooperative RNs which operate with half-duplex and DF. The system model comprises an AP, two IDs, and K RNs in the absence of a direct link between the IDs and AP, as shown in Fig. 1. In massive IoT networks, we may consider the communication scenario where three or more IDs attempt to send their packets over the same time-frequency radio resources simultaneously. However, the decoding complexity of the JD algorithm exponentially increases at each RN and the receiver as the number of devices increases. Moreover, the SIC decoding technique results in worse outage performance even in the high SNR regime because of error propagation as the number of devices increases. Thus, a two-device uplink NOMA scenario is commonly investigated in the literature by assuming that many IDs are separated into several small groups using orthogonal radio resources, user clustering, etc. [41], [42], [43]. In this article, we also focus on the uplink NOMA system with two IDs. We assume that the AP is equipped with M multiple antennas, whereas the RNs and IDs have a single antenna. The notation $h_{sk}[n]$ denotes the channel coefficient in phase n from ID s ($s \in \{1, 2\}$) to RN k ($k \in \{1, 2, \ldots, K\}$) in the first hop comprising an ID-to-RN (I2R) link, and $\mathbf{h}_{k\mathsf{a}}[n]$ denotes the channel coefficient vector in phase n from RN k to AP in the second hop, where there are RN-to-AP (R2A) links. Let the index of the selected RN forwarding the received signal be k^*. The inter-RN interference channel from RN k^* to RN k in phase n is denoted by $h_{\mathrm{I},k^*k}[n]$. All small-scale fading channels are assumed to follow an identically and independently distributed complex Gaussian distribution with zero mean and unit variance, i.e., the Rayleigh fading channel. The distances d_{sk}, $d_{k\mathsf{a}}$, and d_{k^*k} denote those between ID s and RN k, between RN k and AP, and between RN k^* and RN k, respectively. For simplicity of analysis, we assume that $d_{sk} = d_{s\mathsf{r}}$, $d_{k\mathsf{a}} = d_{\mathsf{ra}}$, and $d_{k^*k} = d_{\mathsf{r}}$ regardless of the index k. We define the notation of each channel gain as follows:

$$
\begin{aligned}
g_{sk}[n] &:= d_{s\mathsf{r}}^{-\alpha}|h_{sk}[n]|^2 = \beta_s|h_{sk}[n]|^2 \\
g_{\mathrm{I},k^*k}[n] &:= d_{\mathsf{r}}^{-\alpha}\left|h_{\mathrm{I},k^*k}[n]\right|^2 = \beta_{\mathsf{r}}\left|h_{\mathrm{I},k^*k}[n]\right|^2 \\
g_{k\mathsf{a}}[n] &:= d_{\mathsf{ra}}^{-\alpha}\|\mathbf{h}_{k\mathsf{a}}[n]\|^2 = \beta_{\mathsf{ra}}\|\mathbf{h}_{k\mathsf{a}}[n]\|^2 \\
g_{k^*\mathsf{a}}[n] &:= d_{\mathsf{ra}}^{-\alpha}\|\mathbf{h}_{k^*\mathsf{a}}[n]\|^2 = \beta_{\mathsf{ra}}\|\mathbf{h}_{k^*\mathsf{a}}[n]\|^2
\end{aligned}
$$

where α denotes the path-loss exponent. The instantaneous received signal-to-noise ratio (SNR) is denoted by $P_s g_{sk}[n]/N_0 = \rho_s g_{ks}[n]$, $P_{\mathsf{r}} g_{\mathrm{I},k^*k}[n]/N_0 = \rho_{\mathsf{r}} g_{\mathrm{I},k^*k}[n]$, and $P_{\mathsf{r}} g_{k^*\mathsf{a}}[n]/N_0 = \rho_{\mathsf{r}} g_{k^*\mathsf{a}}[n]$ where P_w is the transmit power of node w ($w \in \{1, 2, \mathsf{r}\}$). The node w denotes the ID i for $w \in \{1, 2\}$ and the RN for $w = \mathsf{r}$. The term N_0 denotes power of the noise. The transmitted signal at node w is denoted by x_w with unit power, i.e., $\mathbb{E}[|x_w|^2] = 1$. We assume that the additive white Gaussian noise (AWGN) follows a complex Gaussian distribution with zero mean and N_0 variance. Local channel state information at the receiver (CSIR) is assumed, which is widely adopted in literature [44], [45].

We now explain the common operations of the existing and proposed schemes. In the I2R link, both IDs transmit signals to all RNs simultaneously over the same subcarrier. Each RN then receives the signals and decodes them. We define an index set $\mathcal{D}[n]$ that includes the index of RNs that successfully decode the received signal in phase n. In the R2A link, we consider only a single relay selection scheme based on the maximum channel gain criterion as follows:

$$
k^* = \underset{k \in \mathcal{D}[n]}{\arg\max} \|\mathbf{h}_{k\mathsf{a}}[n]\|^2. \tag{2}
$$

The difference between the two schemes is the period of the transmissions in both links: one transmission in every phase in both links simultaneously for the proposed technique, whereas there is one transmission in each hop separately for the two phases in the existing scheme. Details of each scheme are described in the following sections. For clearly, $\log(\cdot)$ denotes the logarithm of bases 2, $\log_2(\cdot)$, in this article.

A. Existing Two-Hop Uplink Cooperative NOMA Scheme

In this section, we explain the two-hop half-duplex uplink NOMA scheme as a reference. In this scheme, the signals are transmitted via the I2R link in the first phase ($n = 1$). Then, the RN k^* forwards the received signals via the R2A link in the second phase ($n = 2$) as shown in Fig. 2. Then, this relaying

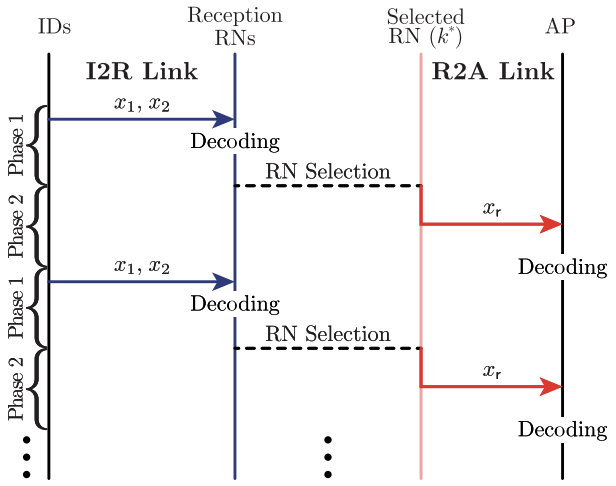

Fig. 2. Timing diagram of the two-hop uplink cooperative NOMA scheme with half-duplex RNs.

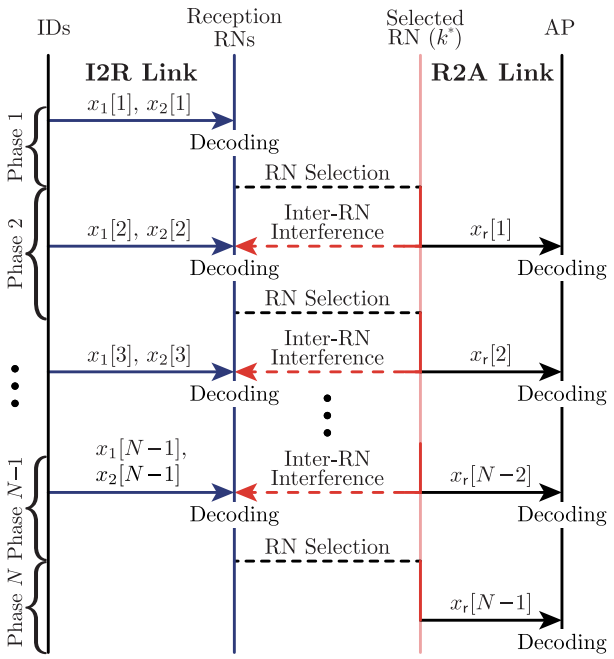

Fig. 3. Timing diagram of the proposed uplink cooperative NOMA protocol with half-duplex RNs.

procedure is repeated for subsequent signals. For convenience, we drop the phase index for this scheme.

In the first phase, the received signal at RN k is given by

$$y_k = \sqrt{P_1 d_{1\mathsf{r}}^{-\alpha}} h_{1k} x_1 + \sqrt{P_2 d_{2\mathsf{r}}^{-\alpha}} h_{2k} x_2 + z_k \tag{3}$$

where z_k denotes AWGN at RN k. It is assumed that each RN decodes the signal by the JD technique. Then, the event of successful decoding at RN k is given by [35] and [46]

$$\mathscr{E}_{\mathsf{r}}^{\text{Two-hop}} = \left\{ \begin{array}{l} \frac{1}{2}\log(1+\rho_1 g_{1k}) \geq R_1 \ \bigcap \\ \frac{1}{2}\log(1+\rho_2 g_{2k}) \geq R_2 \ \bigcap \\ \frac{1}{2}\log(1+\rho_1 g_{1k}+\rho_2 g_{2k}) \geq R_1+R_2 \end{array} \right\} \tag{4}$$

where R_s $(s = 1, 2)$ denotes the transmission rate of ID s and $\rho_s g_{sk} = P_s d_{s\mathsf{r}}^{-\alpha} |h_{sk}|^2 / N_0$. It is worth noting that the spectral efficiency becomes reduced by half due to the duty-cycle loss of half-duplex RNs. An RN is selected to forward the received signal among the RNs satisfying (2).

In the second phase $(n = 2)$, the selected RN k^* transmits the successfully decoded signal x_{r} to the AP. Then, the AP receives the signal given by

$$y_{\mathsf{a}} = \sqrt{P_{\mathsf{r}} d_{\mathsf{ra}}^{-\alpha}} \mathbf{h}_{k^*\mathsf{a}} x_{\mathsf{r}} + z_{\mathsf{a}} \tag{5}$$

where $x_{\mathsf{r}} = \sqrt{a_1} x_1 + \sqrt{a_2} x_2$ $(a_1 + a_2 = 1)$ and z_{a} denotes the AWGN at the AP. The event of successful decoding the AP is expressed as follows:

$$\mathscr{E}_{\mathsf{a}}^{\text{Two-hop}} = \left\{ \frac{1}{2}\log(1+\rho_{\mathsf{r}} g_{k^*\mathsf{a}}) \geq R_1 + R_2 \right\} \tag{6}$$

where $\rho_{\mathsf{r}} g_{k^*\mathsf{a}} = P_{\mathsf{r}} d_{\mathsf{ra}}^{-\alpha} \|\mathbf{h}_{k^*\mathsf{a}}\|^2 / N_0$.

B. Proposed Spectrally Efficient Cooperative NOMA Protocol

Fig. 3 describes the overall procedure of the proposed spectrally efficient uplink cooperative NOMA protocol. The selected RN sends the received signal to the AP while the other RNs receive signals from both IDs at the same time. The selected RN cannot receive the signal from both IDs while transmitting signals because it operates with half-duplex. Hence, the proposed protocol achieves nearly twice spectral efficiency compared with the existing two-hop cooperative NOMA scheme, but it may suffer from inter-RN interference.

The received signal at RN k $(k \neq k^*)$ in the nth transmission phase $(n = 1, \ldots, N-1)$ is given by

$$y_k[n] = \underbrace{\sqrt{P_1 d_{1\mathsf{r}}^{-\alpha}} h_{1k}[n] x_1[n] + \sqrt{P_2 d_{2\mathsf{r}}^{-\alpha}} h_{2k}[n] x_2[n]}_{\text{Desired signals}} + \underbrace{\sqrt{P_{\mathsf{r}} d_{\mathsf{r}}^{-\alpha}} h_{\mathrm{I},k^*k}[n] x_{\mathsf{r}}[n-1]}_{\text{Inter-relay interference signal}} + z_k[n] \tag{7}$$

where $x_{\mathsf{r}}[0] = 0$. The method to deal with the inter-RN interference at each RN differs according to whether the RN succeeds to decode the received signal in the previous phase. RNs that successfully decode the received signal belonging to $\mathcal{D}[n-1]$ can perfectly cancel the inter-RN interference under local CSI assumption. Therefore, the received signal at RN k such that $k \in \mathcal{D}[n-1]$ is represented by $y_k[n] = \sqrt{P_1 d_{1\mathsf{r}}^{-\alpha}} h_{1k}[n] x_1[n] + \sqrt{P_2 d_{2\mathsf{r}}^{-\alpha}} h_{2k}[n] x_2[n] + z_k[n]$. Subsequently, under the JD strategy, the event of successful decoding at the nth phase for the RNs included in the decoding set is given by

$$\mathscr{E}_{\mathsf{r},1}^{\text{Prop.}} = \left\{ \begin{array}{l} \frac{N-1}{N}\log(1+\rho_1 g_{1k}[n]) \geq R_1 \ \bigcap \\ \frac{N-1}{N}\log(1+\rho_2 g_{2k}[n]) \geq R_2 \ \bigcap \\ \frac{N-1}{N}\log(1+\rho_1 g_{1k}[n]+\rho_2 g_{2k}[n]) \geq R_1+R_2 \end{array} \right\}. \tag{8}$$

However, RNs that fail to decode the received signal cannot cancel the inter-RN interference signal. Then, such RNs tries

to decode the received signals under the inter-RN interference. We exploit the JD strategy which is widely used to increase the decoding performance under the presence of interference. It has been well-known that the JD strategy outperforms the SIC strategy in MACs in terms of both throughput and error performances [46]. At the nth phase of the proposed protocol, RN k ($k \notin \mathcal{D}[n-1]$, $k \neq k^*$) tries to decode multiple signals from two IDs ($x_1[n]$ and $x_2[n]$) and the selected RN ($x_{\mathsf{r}}[n-1]$). The condition of successful decoding based on capacity region for this case is given by [35]

$$\mathscr{E}_{\mathsf{r},2}^{\text{Prop.}} = \left\{ \begin{array}{l} \log\left(1+\sum_{w\in\mathcal{W}} q_w\right) \geq \frac{N\sum_{w\in\mathcal{W}} R_w}{N-1}, \\ \qquad\qquad \forall \mathcal{W} \subseteq \{1,2,\mathsf{r}\}, \text{ and } \mathcal{W} \neq \{\mathsf{r}\} \end{array} \right\} \tag{9}$$

where $q_1 = \rho_1 g_{1k}[n]$, $q_2 = \rho_2 g_{2k}[n]$, $q_{\mathsf{r}} = \rho_{\mathsf{r}} g_{\mathsf{I},k^*k}[n]$, and $R_{\mathsf{r}} = R = R_1 + R_2$. In (9), when $\mathcal{W} = \{\mathsf{r}\}$, only the interference signal is decoded successfully. Thus, this case is not included in the successful decoding condition.

Simultaneously, the received signal at the AP is given by $y_{\mathsf{a}}[n] = \sqrt{P_{\mathsf{r}} d_{\mathsf{ra}}^{-\alpha}}\mathbf{h}_{k^*\mathsf{a}}[n]x_{\mathsf{r}}[n-1] + z_{\mathsf{a}}[n]$ ($n = 2, 3, \ldots, N$). The event of successful decoding at the AP is given by

$$\mathscr{E}_{\mathsf{a}}^{\text{Prop.}} = \left\{ \frac{N-1}{N} \log(1+\rho_{\mathsf{r}} g_{k^*\mathsf{a}}[n]) \geq R_1 + R_2 \right\}. \tag{10}$$

C. Proposed Protocol With More Than Two IDs

Although we focus on the two-ID scenario for uplink cooperative NOMA systems in the previous section, the proposed protocol can be applied to the case with more than two IDs. When there exist S IDs, the received signal at RN k ($k \neq k^*$) in the nth transmission phase ($n = 1, \ldots N-1$) is given by

$$\begin{aligned} y_k[n] = &\sum_{s=1}^{S} \sqrt{P_s d_{s\mathsf{r}}^{-\alpha}} h_{sk}[n] x_s[n] \\ &+ \sqrt{P_{\mathsf{r}} d_{\mathsf{r}}^{-\alpha}} h_{\mathsf{I},k^*k}[n] x_{\mathsf{r}}[n-1] + z_k[n] \end{aligned} \tag{11}$$

where the subscript s denotes the sth ($s \in \{1, 2, \ldots, S\}$) ID. Then, the successful decoding condition without the inter-RN interference signal is generalized from (8) as follows:

$$\begin{aligned} \mathscr{E}_{\mathsf{r},1}^{\text{Prop.}} = \Bigg\{ &\log\left(1+\sum_{w\in\mathcal{W}} q_w\right) \\ &\geq \frac{N\sum_{w\in\mathcal{W}} R_w}{N-1} \quad \forall \mathcal{W} \subseteq \{1,2,\ldots,S\} \Bigg\}. \end{aligned} \tag{12}$$

The successful decoding condition with an inter-RN interference signal is given by

$$\mathscr{E}_{\mathsf{r},2}^{\text{Prop.}} = \left\{ \begin{array}{l} \log\left(1+\sum_{w\in\mathcal{W}} q_w\right) \geq \frac{N\sum_{w\in\mathcal{W}} R_w}{N-1}, \\ \qquad\qquad \forall \mathcal{W} \subseteq \{1,2,\ldots,S,\mathsf{r}\} \text{ and } \mathcal{W} \neq \{\mathsf{r}\} \end{array} \right\} \tag{13}$$

where R_{r} is defined as $\sum_{s=1}^{S} R_s$. Through the relay selection process and the decoding process at each relay, the selected relay sends a signal to the AP at the second hop. At the AP, the condition of successful decoding is given by

$$\mathscr{E}_{\mathsf{a}}^{\text{Prop.}} = \left\{ \frac{N-1}{N} \log(1+\rho_{\mathsf{r}} g_{k^*\mathsf{a}}[n]) \geq \sum_{s=1}^{S} R_s \right\}. \tag{14}$$

Unfortunately, we cannot mathematically analyze the outage probability of the proposed protocol when there exist more than two IDs.

III. Performance Analysis

In this section, we mathematically analyze the outage probabilities of both existing and proposed cooperative NOMA protocols. We assume that the transmission power of all nodes is the same as each other as $\rho = \rho_1 = \rho_2 = \rho_{\mathsf{r}}$.

A. Outage Probability of Two-Hop Uplink NOMA Scheme

In this section, we derive the closed-form outage probability of the existing two-hop half-duplex uplink NOMA scheme described in Section II-A.

Theorem 1: When there exist K half-duplex DF RNs, the outage probability of the two-hop half-duplex relaying scheme in uplink cooperative NOMA systems without direct link between IDs and AP is given by

$$\begin{aligned} \Pr\{\mathcal{O}\} = &\sum_{u=0}^{K} \left(1 - e^{\frac{2^{2(R_1+R_2)}-1}{\beta_{\mathsf{ra}}\rho}} \sum_{m=0}^{M-1} \left(\frac{2^{2(R_1+R_2)}-1}{\beta_{\mathsf{ra}}\rho}\right)^m \frac{1}{m!}\right)^u \\ &\times \binom{K}{u} p_o^{K-u} (1-p_o)^u \end{aligned} \tag{15}$$

where $\mathcal{O}$ denotes the outage event, M denotes the number of antennas at the AP, and p_o denotes the probability that an RN fails to decode the received signal. To be specific, p_o is given by

$$p_o = \left\{ \begin{array}{ll} 1 - \Phi_2(\beta_1, 2R, 2R_2)\Phi_1(\beta_2, 2R_2) & \\ -\Phi_1(\beta_2, 2R)\frac{1}{\beta_1}\frac{1}{\frac{1}{\beta_1}-\frac{1}{\beta_2}}[\Phi_3(\beta_1,\beta_2,2R_1) & \\ -\Phi_4(\beta_1,\beta_2,2R,2R_2)], & \text{if } \beta_1 \neq \beta_2 \\ 1 - \Phi_2(\beta_1, 2R, 2R_2)\Phi_1(\beta_2, 2R_2) & \\ -\Phi_1(\beta_2, 2R)\frac{1}{\beta_1}\frac{(2^{2R_1}-1)(2^{2R_2}-1)}{\rho}, & \text{if } \beta_1 = \beta_2 \end{array} \right. \tag{16}$$

where $R = R_1 + R_2$, $\Phi_1(\gamma_1, \mu) \triangleq e^{-(1/\gamma_1)(2^{\mu}-1)/\rho}$, $\Phi_2(\gamma_1, \mu, \omega) \triangleq e^{-(1/\gamma_1)(2^{\mu}-2^{\omega})/\rho}$, $\Phi_3(\gamma_1, \gamma_2, \mu) \triangleq e^{-(1/\gamma_1 - 1/\gamma_2)(2^{\mu}-1)/\rho}$, and $\Phi_4(\gamma_1, \gamma_2, \mu, \omega) \triangleq e^{-(1/\gamma_1 - 1/\gamma_2)(2^{\mu}-2^{\omega})/\rho}$.

Proof: Refer to Appendix A. ∎

B. Outage Probability of Spectrally Efficient Cooperative NOMA Protocol

In this section, we mathematically analyze the proposed uplink cooperative NOMA protocol in terms of outage probability.

Theorem 2: When there exist K half-duplex RNs, the outage probability of the proposed uplink cooperative NOMA protocol without direct link between the two IDs and AP is given by

$$\Pr\{\mathcal{O}\} = \sum_{u=0}^{K} \left[1 - e^{-\frac{2^{\frac{N(R_1+R_2)}{N-1}}-1}{\beta_{\mathsf{ra}}\rho}} \sum_{m=0}^{M-1} \left(\frac{2^{\frac{N(R_1+R_2)}{N-1}}-1}{\beta_{\mathsf{ra}}\rho}\right)^m \frac{1}{m!} \right]^u \pi_u \tag{17}$$

TABLE I
SOLUTIONS OF VALUES OF Q_w ACCORDING TO VALUE OF β_w

	Q_M	Q_m	Q_{r}
$\beta_m > \beta_{\mathsf{r}}$	$2^{2R'}-2^{R'_m+R'}$	$2^{R'_m+R'}-1$	0
$\beta_M > \beta_{\mathsf{r}} \geq \beta_m$	$2^{2R'}-2^{R'_m+R'}$	$2^{R'_m}-1$	$2^{R'_m+R'}-2^{R'_m}$
$\beta_{\mathsf{r}} \geq \beta_M$	$2^{R'}-2^{R'_m}$	$2^{R'_m}-1$	$2^{2R'}-2^{R'}$

where π_u ($u \in \{0, 1, \ldots, K\}$) denotes the stationary distribution regarding the number of RNs that succeed in decoding and $\sum_{u=0}^{K} \pi_u = 1$.

Proof: Refer to Appendix B. ■

Corollary 1: When $K = 3$, the outage probability of the proposed protocol given in (17) is rewritten as follows:

$$\Pr\{\mathcal{O}\} = \sum_{u=0}^{3}\left[1 - e^{-\frac{2^{\frac{N(R_1+R_2)}{N-1}}-1}{\beta_{\mathsf{ra}}\rho}} \sum_{m=0}^{M-1}\left(\frac{2^{\frac{N(R_1+R_2)}{N-1}}-1}{\beta_{\mathsf{ra}}\rho}\right)^m \frac{1}{m!}\right]^u \pi_u \tag{18}$$

where $\pi_0 = (P_{2,0}+P_{1,0}P_{2,1}-P_{1,1}P_{2,0})/[(P_{2,0}-P_{1,0})\{P_{0,1}+P_{3,1}P_{0,3}-P_{2,1}(1+P_{0,3})\}+(P_{1,1}-P_{2,1}-1)\{P_{0,0}+P_{3,0}P_{0,3}-P_{2,0}(1+P_{0,3})-1\}]$, $\pi_1 = ([\{P_{0,0}+P_{3,0}P_{0,3}-P_{2,0}(1+P_{0,3})-1\}\pi_0 + P_{2,0}]/[P_{2,0} - P_{1,0}])$, $\pi_2 = 1 - \{(1 + P_{0,3})\pi_0 + \pi_1\}$, $\pi_3 = P_{0,3}\pi_0$.

Proof: By substituting $K = 3$ into (17) and solving $\boldsymbol{\pi} = \mathbf{P}_3\boldsymbol{\pi}$, (18) can be readily obtained. ■

C. Upper Bound of Outage Probability of Spectrally Efficient Cooperative NOMA Protocol

In the previous section, we derive the exact outage probability of the proposed uplink cooperative NOMA protocol. However, the exact expression of the outage probability is somewhat complicated due to effect of the inter-RN interference. To obtain an insight from the outage probability, we provide a simple upper bound of the outage probability of the proposed uplink cooperative NOMA protocol by simplifying the condition of successful decoding at RNs with or without interference from other RNs. In this section, we only deal with the case of RN with inter-RN interference since it is a general case including the case without interference as a special case.

Theorem 3: An upper bound of the outage probability of the proposed technique is derived by substituting an upper bound of the outage probability at RN with inter-RN interference (19) instead of $p_{o,\mathrm{I}}$ in (30)

$$p_{o,\mathrm{I}} \leq \bar{p}_{o,\mathrm{I}} = 1 - \exp\left(-\frac{1}{\rho}\left(\frac{1}{\beta_1}Q_1 + \frac{1}{\beta_2}Q_2 + \frac{1}{\beta_{\mathsf{r}}}Q_{\mathsf{r}}\right)\right) \tag{19}$$

where Q_1, Q_2, and Q_{r} are given in Table I where the subscripts m and M ($m, M \in \{1, 2\}$, $m \neq M$) denote

$$M = \arg\max_{s\in\{1,2\}} \beta_s \quad \text{and} \quad m = \arg\min_{s\in\{1,2\}} \beta_s$$

respectively.

Proof: Refer to Appendix C. ■

D. Diversity Order of Spectrally Efficient Cooperative NOMA Protocol

In this section, we mathematically analyze a diversity order of the proposed spectrally efficient uplink cooperative NOMA protocol. The diversity order is widely used to observe the tendency of the outage probability in the high SNR regime and it is formally defined as follows:

$$\eta = -\lim_{\rho\to\infty} \frac{\log \Pr\{\mathcal{O}\}}{\log \rho}. \tag{20}$$

Theorem 4: The diversity order of the proposed uplink cooperative NOMA protocol with K half-duplex RNs achieves $K - 1$ regardless of the number of antennas at the AP

$$\eta = K - 1.$$

Proof: Refer to Appendix D. ■

The diversity order is closely related to the number of relay candidates for the second hop transmission which is equal to the cardinality of the decoding set. In the proposed protocol, a single RN is selected to forward the received signal and it is excluded from the decoding set because of the half-duplex operation. Although the diversity order of the proposed cooperative NOMA protocol is reduced by one compared with the conventional half-duplex cooperative NOMA scheme, the performance of the proposed technique is significantly improved by removing the duty-cycle loss.

IV. NUMERICAL RESULTS

In this section, we evaluate performances of the proposed uplink cooperative NOMA protocol, and compare them with the existing scheme in terms of the outage probability and effective throughput. Moreover, we validate the mathematical analysis derived in this article by showing that they coincide with computer simulations. The terms "Proposed" and "Two-hop" in figures of this section stand for the proposed spectrally efficient cooperative NOMA protocol and the existing two-hop half-duplex uplink cooperative NOMA scheme. For simulations, we follow common assumptions that have been widely used in similar studies in order to fairly compare the proposed protocol with existing schemes. The target rates, R_1 and R_2, are set to 1 bps/Hz and the path-loss exponent is 3.

Figs. 4 and 5 show that the outage probability of the conventional two-hop uplink cooperative NOMA scheme and the proposed spectrally efficient cooperative NOMA protocol according to d_1 for varying SNR, respectively, when $K = 3$, $M = 5$, and $d_2 = d_{\mathsf{ra}} = 1$. It is worth noting that d_1 indicates the relative distance compared with the aforementioned distances as a unit. Figs. 4 and 5 show that the JD technique significantly outperforms the SIC scheme both in the conventional and the proposed cooperative uplink NOMA protocols. The SIC scheme yields an error floor in high SNR regimes as expected. In Figs. 4 and 5, it is confirmed that the analytical results match well with the Monte-Carlo simulation results.

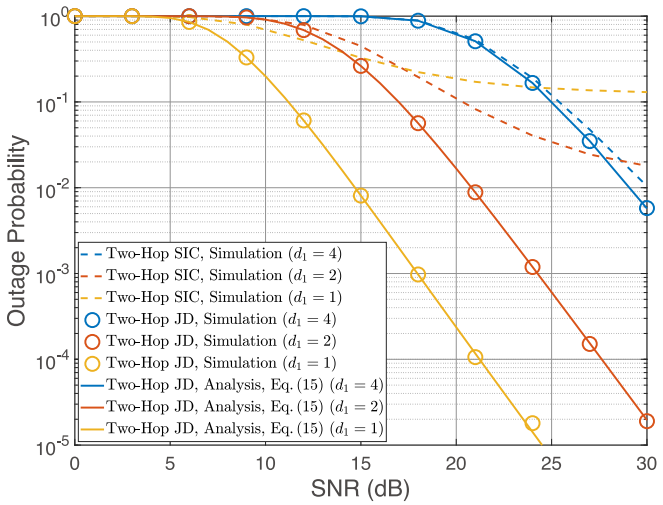

Fig. 4. Outage probability of the conventional two-hop uplink cooperative NOMA scheme according to d_1 when $K = 3$, $M = 5$, $R_1 = R_2 = 1$, and $d_2 = d_{\mathsf{ra}} = 1$.

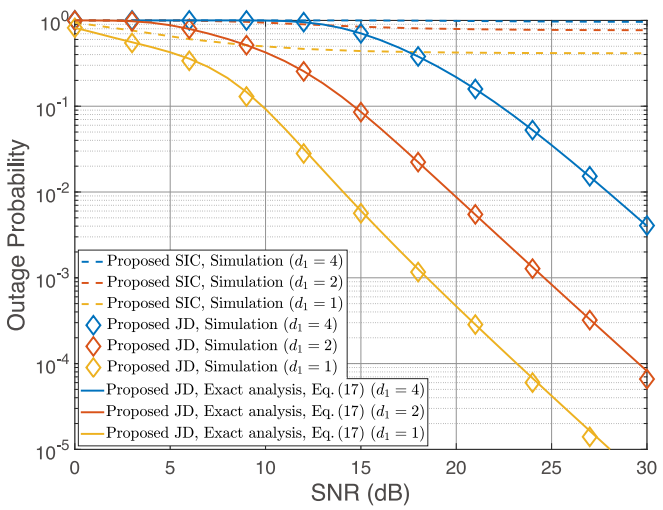

Fig. 5. Outage probability of the proposed spectrally efficient uplink cooperative NOMA protocol according to d_1 when $K = 3$, $M = 5$, $R_1 = R_2 = 1$, and $d_2 = d_{\mathsf{r}} = d_{\mathsf{ra}} = 1$.

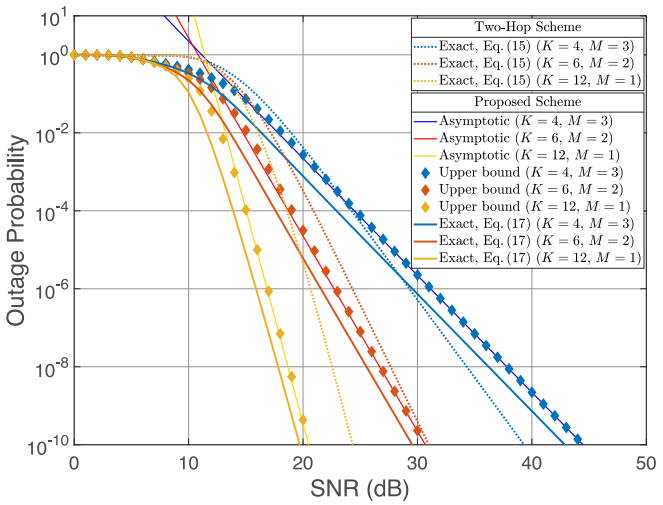

Fig. 6. Outage probability comparison between the conventional two-hop cooperative NOMA and the proposed spectrally efficient uplink cooperative NOMA protocols for varying K and M when $R_1 = R_2 = 1$, $d_1 = 2$, and $d_2 = d_{\mathsf{r}} = d_{\mathsf{ra}} = 1$.

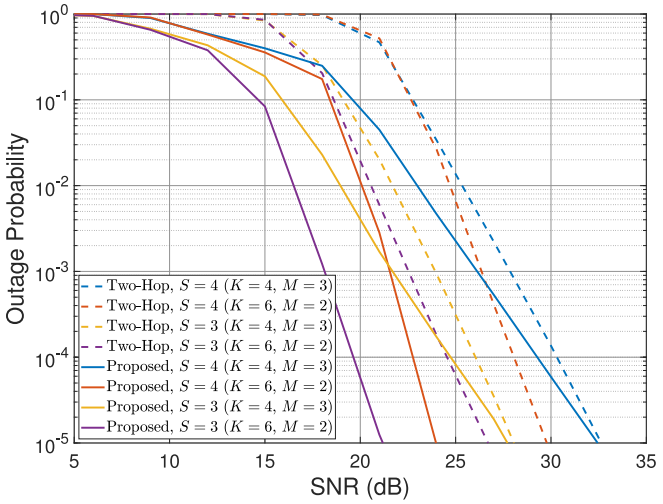

Fig. 7. Outage probability comparison between the conventional two-hop and the proposed spectrally efficient uplink cooperative NOMA protocols with respect to S when $R_s = 1$ ($s \in \{1, 2, \ldots, S\}$), $d_{\mathsf{r}} = d_{\mathsf{ra}} = 1$ and $(K, M) = \{(4, 3), (6, 2)\}$.

Fig. 6 compares the outage probability of the proposed cooperative NOMA protocol with the existing scheme. In particular, the derived exact analysis, the upper bound of the exact analysis, and the asymptotic analysis are compared. It is shown that the proposed protocol outperforms the conventional two-hop scheme in terms of the outage probability over all SNR regimes when $K = 12$, 6. When $K = 4$, the proposed technique yields better outage performance if the SNR is smaller than 28 dB. The performance gap between the proposed and conventional protocols becomes smaller or reversed as the SNR increases due to different diversity gain of the two protocols. The diversity gain of the proposed technique is equal to $K - 1$, whereas that of the conventional scheme is equal to K. It is worth noting that the proposed protocol outperforms the conventional two-hop protocol in practical wireless system environments where $K \geq 4$ and the required packet error rate[1] is set to 10^{-5}. We also observe that the upper bound and the asymptotic analysis of the outage probability of the proposed protocol well characterize the exact analysis especially when the SNR becomes high.

Fig. 7 compares the outage probability of the proposed spectrally efficient cooperative NOMA protocol with the existing two-hop scheme for various system parameters when there exist more than two IDs. When $S = 3$, it is assumed that $(d_1, d_2, d_3) = (1, 1.5, 2)$. When $S = 4$, it is assumed that $(d_1, d_2, d_3, d_4) = (1, 1, 2, 2)$. It is shown that the proposed protocol also outperforms the existing two-hop scheme even when the number of IDs increases.

[1]The required packet error rate for ultrareliable low-latency communication (URLLC) has been reported in [47].

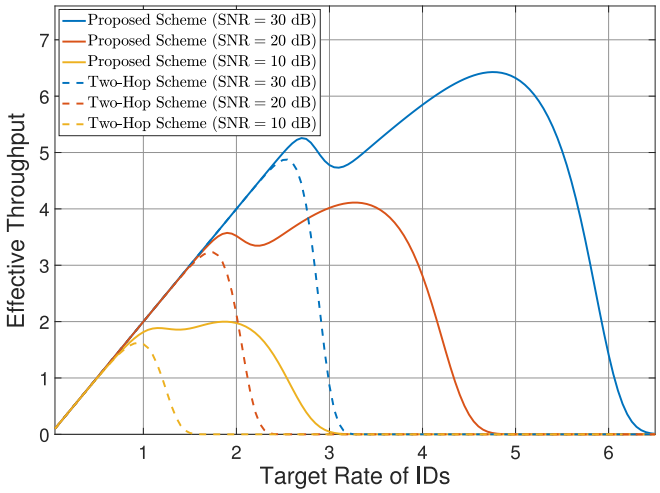

Fig. 8. Effective throughput comparison between the conventional two-hop and the proposed spectrally efficient uplink cooperative NOMA protocols according to SNR when $K = 3$, $M = 5$, and $d_1 = d_2 = d_{\mathsf{r}} = d_{\mathsf{ra}} = 1$.

Fig. 8 compares the effective throughput performance of the proposed spectrally efficient cooperative NOMA protocol with the existing two-hop scheme according to the target rate of IDs with various SNR values. The effective throughput is defined as follows:

$$\text{Effective Throughput} = (R_1 + R_2)(1 - \Pr\{\mathcal{O}\}). \quad (21)$$

In the low target-rate regime, both the proposed and the conventional protocols result in similar performances. As the target rate increases, the proposed protocol significantly outperforms the existing scheme in terms of the effective throughput. Note that the maximum achievable effective throughput of the proposed protocol is also significantly higher than that of the existing scheme.

V. Conclusion

In this article, we considered an uplink cooperative NOMA system comprising two transmitting IDs, a single AP, and K half-duplex DF RNs. In particular, we proposed a spectrally efficient relaying protocol by assuming the absence of a direct link between the IDs and the AP. As a main result, we mathematically derived a closed-form expression of the outage probability of not only the proposed cooperative relaying protocol but also the existing relaying scheme. We also validated the analytical results through extensive computer simulations. To the best of our knowledge the mathematical analysis obtained in this article is the first analytical result reported in the literature. It is worth noting that the proposed cooperative NOMA framework outperforms two-hop half-duplex cooperative NOMA in terms of outage probability and effective throughput. Our analytical framework can be easily extended for the downlink cooperative NOMA system since the uplink cooperative NOMA signal model can be regarded as a generalized signal model of the downlink model. Therefore, we believe that the proposed protocol is expected to be a promising technical candidate for 6G wireless massive IoT networks.

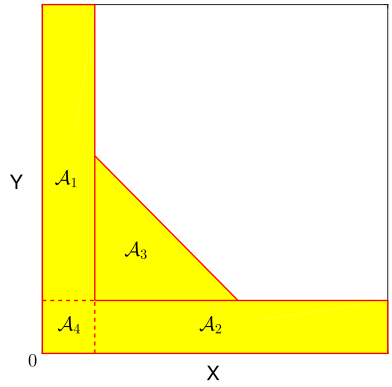

Fig. 9. Total outage region of the RN in two-hop uplink cooperative NOMA scheme.

Appendix A
Proof of Theorem 1

The outage probability of the two-hop half-duplex relaying scheme can be formulated using the total probability theorem as follows:

$$\begin{aligned}\Pr\{\mathcal{O}\} &= \sum_{u=0}^{K} \Pr\{\mathcal{O} \mid |\mathcal{D}| = u\} \Pr\{|\mathcal{D}| = u\} \\ &= \sum_{u=0}^{K} \left(\Pr\left\{g_{k^*\mathsf{a}} < \frac{2^{2(R_1+R_2)} - 1}{\rho}\right\}\right)^u \Pr\{|\mathcal{D}| = u\} \quad (22)\end{aligned}$$

where $\Pr\{\mathcal{O} \mid |\mathcal{D}| = 0\} = 1$ and $|\{\cdot\}|$ denotes the cardinality of a set. In order to calculate the outage probability at AP for given $|\mathcal{D}|$, i.e., the second term of (22), we derive the cumulative density function (CDF) of the channel gain between the selected RN and the AP. This is because the channel gain $g_{k\mathsf{a}} := \beta_{\mathsf{ra}} \|\mathbf{h}_{k\mathsf{a}}\|^2$ in the system model, $g_{k\mathsf{a}}$ follows the Erlang distribution, i.e., $g_{k\mathsf{a}} \sim \text{Erlang}(M, 1/\beta_{\mathsf{ra}})$ ($k \in 1, 2, \ldots, K$) [36]. Therefore, the CDF of the largest order statistics for a given $|\mathcal{D}| = u$ is $F_{g_{k^*\mathsf{a}}}(x) = \{F_{g_{k\mathsf{a}}}(x)\}^u$, where $F_{g_{k\mathsf{a}}}(x)$ denotes the CDF of the Erlang distribution

$$\begin{aligned}\Pr\{\mathcal{O} \mid |\mathcal{D}| = u\} &= \left\{F_{g_{k^*\mathsf{a}}}\left(\frac{2^{2(R_1+R_2)} - 1}{\rho}\right)\right\}^u \\ &= \left\{1 - e^{-\frac{2^{2(R_1+R_2)}-1}{\beta_{\mathsf{ra}}\rho}} \sum_{m=0}^{M-1} \frac{1}{m!}\left(\frac{2^{2(R_1+R_2)} - 1}{\beta_{\mathsf{ra}}\rho}\right)^m\right\}^u \quad (23)\end{aligned}$$

where $F_{g_{k^*\mathsf{a}}}(x) = 1 - e^{-x/\beta_{\mathsf{ra}}} \sum_{m=0}^{M-1} (x/\beta_{\mathsf{ra}})^m/(m!)$ is the CDF of the random variable $g_{k^*\mathsf{a}}$, which follows an Erlang distribution with mean $M\beta_{\mathsf{ra}}$ and variance $M\beta_{\mathsf{ra}}^2$. The second term of (22) can be represented as $\Pr\{|\mathcal{D}| = u\} = \binom{K}{u} p_o^{K-u}(1-p_o)^u$.

To obtain the closed-form of p_o, we visualize the outage region on the coordinate axis that is related to the channel gains between the IDs and the RN, as shown in Fig. 9. In other words, variables X and Y in Fig. 9 denote the g_{1k} and g_{2k}, respectively. We compute the areas of four outage regions, $\mathcal{A}_1$, $\mathcal{A}_2$, $\mathcal{A}_3$, and $\mathcal{A}_4$, to obtain the closed-form of $p_o = \mathcal{A}_1 + \mathcal{A}_2 + \mathcal{A}_3 - \mathcal{A}_4 = \mathcal{A}$, and the integral can be calculated as follows:

$$p_o = \iint_{\mathcal{A}} f_{g_{1k},g_{2k}}(x, y)dydx$$

$$= \sum_{a=1}^{3} \iint_{\mathcal{A}_a} \frac{1}{\beta_1} e^{-\frac{1}{\beta_1}x} \frac{1}{\beta_2} e^{-\frac{1}{\beta_2}y} dydx - \iint_{\mathcal{A}_4} \frac{1}{\beta_1} e^{-\frac{1}{\beta_1}x} \frac{1}{\beta_2} e^{-\frac{1}{\beta_2}y} dydx \quad (24)$$

where $f_W(w)$ is the probability density function of W for the random variable w. The g_{1k} and g_{2k} follow an exponential distribution with mean β_1 and β_2, respectively. According to the condition of the distances between both IDs and RN, (24) is solved differently. For example, $\mathcal{A}_3$ is formulated as follows:

$$\begin{aligned}
&\iint_{\mathcal{A}_3} \frac{1}{\beta_1} e^{-\frac{1}{\beta_1}x} \frac{1}{\beta_2} e^{-\frac{1}{\beta_2}y} dydx \\
&= \int_{\frac{2^{2R_1}-1}{\rho}}^{\frac{2^{2R_2}\left(2^{2R_1}-1\right)}{\rho}} \frac{1}{\beta_1} e^{-\frac{1}{\beta_1}x} \int_{\frac{2^{2R_2}-1}{\rho}}^{-x+\frac{2^{2R_1+2R_2}-1}{\rho}} \frac{1}{\beta_2} e^{-\frac{1}{\beta_2}y} dydx \\
&= \int_{\frac{2^{2R_1}-1}{\rho}}^{\frac{2^{2R_2}\left(2^{2R_1}-1\right)}{\rho}} \Bigg[\frac{1}{\beta_1} e^{-\frac{1}{\beta_1}x} e^{-\frac{1}{\beta_2}\frac{2^{2R_2}-1}{\rho}} \\
&\qquad - \underbrace{\frac{1}{\beta_1} e^{-\left(\frac{1}{\beta_1}-\frac{1}{\beta_2}\right)x}}_{\mathcal{T}} e^{-\frac{1}{\beta_2}\frac{2^{2R_1+2R_2}-1}{\rho}} \Bigg] dx.
\end{aligned} \quad (25)$$

In (25), $\mathcal{T}$ is equal to $1/\beta_1$ when $\beta_1 = \beta_2$ ($d_{1\mathsf{r}} = d_{2\mathsf{r}}$) and then, the calculation of the integral differs from the case when $\beta_1 \neq \beta_2$. After calculating the integral considering the two aforementioned distance cases, we obtain p_o when $\beta_1 \neq \beta_2$ ($d_{1\mathsf{r}} \neq d_{2\mathsf{r}}$), which is given by

$$\begin{aligned}
p_o = 1 &- \Phi_2(\beta_1, 2R, 2R_2)\Phi_1(\beta_2, 2R_2) - \Phi_1(\beta_2, 2R)/\beta_1 \\
&\times \frac{1}{\frac{1}{\beta_1}-\frac{1}{\beta_2}} [\Phi_3(\beta_1, \beta_2, 2R_1) - \Phi_4(\beta_1, \beta_2, 2R, 2R_2)].
\end{aligned} \quad (26)$$

Otherwise, if $\beta \triangleq \beta_1 = \beta_2$

$$\begin{aligned}
p_o = 1 &- \Phi_2(\beta, 2R, 2R_2)\Phi_1(\beta, 2R_2) - \Phi_1(\beta, 2R)/\beta \\
&\times \left(2^{2R_1}-1\right)\left(2^{2R_2}-1\right)/\rho.
\end{aligned} \quad (27)$$

Finally, we obtain the outage probability of the two-hop uplink cooperative NOMA scheme.

APPENDIX B
PROOF OF THEOREM 2

In order to derive the closed-form outage probability in the nth phase, we should consider the dependency among the statuses of the decoding set $\mathcal{D}$ in all the previous phases, contrary to the case of the existing scheme. Since this dependency satisfies Markovity, we can resolve the dependency of the outage probability of the proposed scheme in each phase as shown in the following:

$$\begin{aligned}
\Pr\{\mathcal{O}[n]\} &= \sum_{u=0}^{K} \Pr\{\mathcal{O}[n] \mid |\mathcal{D}[\bar{n}]| = u, \bar{n} = 2, \ldots, n\} \\
&\quad \times \Pr\{|\mathcal{D}[\bar{n}]| = u, \bar{n} = 2, \ldots, n\} \\
&\overset{(a)}{=} \sum_{u=0}^{K} \Pr\{\mathcal{O}[n] \mid |\mathcal{D}[\bar{n}]| = u\} \Pr\{|\mathcal{D}[\bar{n}]| = u\} \\
&= \sum_{u=0}^{K} \left(\Pr\left\{ g_{k^*\mathsf{a}} < \frac{2^{\frac{N(R_1+R_2)}{N-1}} - 1}{\rho} \right\} \right)^u \\
&\quad \times \Pr\{|\mathcal{D}[\bar{n}]| = u\}
\end{aligned} \quad (28)$$

where (a) is derived by the Markovity and $\mathcal{O}[n]$ denotes the outage event in the nth phase. We omit the details of the first term of (28), because it can be obtained in a manner similar to (23). For $\Pr\{|\mathcal{D}[\bar{n}]| = u\}$, we consider a Markov chain that has states related to the cardinality of set $\mathcal{D}$, defined by

$$\mathbf{P}_K = \begin{bmatrix} P_{0,0} & P_{1,0} & \cdots & P_{K,0} \\ \vdots & \vdots & \ddots & \vdots \\ P_{0,K-1} & P_{1,K-1} & \cdots & P_{K,K-1} \\ P_{0,K} & 0 & \cdots & 0 \end{bmatrix} \quad (29)$$

where $P_{i,j}$ denotes the transition probability from state i to j. Note that if any RN successfully decodes the packet in the previous phase, the elements except for $P_{0,K}$ in the last row are zero because the RNs without the transmit RN receive the packet. Each transition probability is formulated as follows:

$$P_{i,j} = \begin{cases} \binom{K}{j} p_o^{K-j}(1-p_o)^j, & \text{if } i = 0 \\ \sum_{x=0}^{\min(i,j)} \binom{i-1}{x} p_o^{i-1-x}(1-p_o)^x & \\ \times \binom{K-i}{j-x} p_{o,\mathrm{I}}^{K-i-j+x}\left(1-p_{o,\mathrm{I}}\right)^{j-x}, & \text{if } i \neq 0 \end{cases} \quad (30)$$

where p_o denotes the outage probability at the RN when it is not affected by inter-RN interference and $p_{o,\mathrm{I}}$ denotes the outage probability at the RN when it is affected by inter-RN interference. The probability p_o is derived as (26) and (27).

To obtain the closed-form of $p_{o,\mathrm{I}}$, we consider the 3-D outage region comprising axes g_{1k}, g_{2k}, and g_{I,k^*k}, as shown in Fig. 10 where the variable Z denotes g_{I,k^*k}, and the outage conditions in Fig. 10(a) are related to the outage events for all $\mathcal{W} \subset \{1, 2, \mathsf{r}\} \neq \{\mathsf{r}\}$. The outage region is calculated by combining $\mathcal{S}_1$, $\mathcal{S}_2$, ..., and $\mathcal{S}_9$. Except for the number of axes in the outage region, the integral is calculated in the same manner as in (26) and (27)

$$\begin{aligned}
p_{o,\mathrm{I}} &= \iiint_{\mathcal{S}} f_{g_{1k},g_{2k},g_{\mathrm{I},k^*k}}(x,y,z)dzdydx \\
&= \sum_{s=1}^{8} \iiint_{\mathcal{S}_s} \frac{1}{\beta_1} e^{-\frac{1}{\beta_1}x} \frac{1}{\beta_2} e^{-\frac{1}{\beta_2}y} \frac{1}{\beta_{\mathsf{r}}} e^{-\frac{1}{\beta_{\mathsf{r}}}z} dzdydx \\
&\quad - \iiint_{\mathcal{S}_9} \frac{1}{\beta_1} e^{-\frac{1}{\beta_1}x} \frac{1}{\beta_2} e^{-\frac{1}{\beta_2}y} \frac{1}{\beta_{\mathsf{r}}} e^{-\frac{1}{\beta_{\mathsf{r}}}z} dzdydx \\
&= \sum_{s=1}^{8} \int_{x_{2,s}}^{x_{1,s}} \frac{1}{\beta_1} e^{-\frac{1}{\beta_1}x} \int_{y_{2,s}}^{y_{1,s}} \frac{1}{\beta_2} e^{-\frac{1}{\beta_2}y} \int_{z_{2,s}}^{z_{1,s}} \frac{1}{\beta_{\mathsf{r}}} e^{-\frac{1}{\beta_{\mathsf{r}}}z} dzdydx \\
&\quad - \int_{x_{2,9}}^{x_{1,9}} \frac{1}{\beta_1} e^{-\frac{1}{\beta_1}x} \int_{y_{2,9}}^{y_{1,9}} \frac{1}{\beta_2} e^{-\frac{1}{\beta_2}y} \int_{z_{2,9}}^{z_{1,9}} \frac{1}{\beta_{\mathsf{r}}} e^{-\frac{1}{\beta_{\mathsf{r}}}z} dzdydx
\end{aligned} \quad (31)$$

where g_{I,k^*k} follows an exponential distribution with mean β_{r}. The outage region $\mathcal{S}_s$ ($\in \{1, 2, \ldots, 9\}$) is represented by the integral range of each channel gain in Table II.

Subsequently, we obtain $p_{o,\mathrm{I}}$ given by (32) and (33), at the bottom of the page, when $\beta_1 \neq \beta_2 \neq \beta_\mathrm{r}$ and $\beta_1 = \beta_2 = \beta_\mathrm{r}$, respectively, where $NR_1/(N-1) = R_1'$, $NR_2/(N-1) = R_2'$, and $NR/(N-1) = R'$.

The transition distribution of $\Pr\{|\mathcal{D}[\bar{n}]| = u\}$, π_u, is derived from the transition matrix $\mathbf{P}_K$. Let $\boldsymbol{\pi} \triangleq [\pi_0 \ \pi_1 \ \ldots \ \pi_K]$. The transition distribution must satisfy the following conditions:

$$\boldsymbol{\pi} = \mathbf{P}_K \boldsymbol{\pi}, \quad \sum_{k=0}^{K} \pi_k = 1. \tag{34}$$

$$\begin{aligned}
p_{o,\mathrm{I}} = {} & \Phi_1(\beta_\mathrm{r}, 2R') \frac{1}{\beta_1\beta_2} \left[\frac{2^{2R'} - 2^{R_1'+R'}}{\rho} \frac{2^{R_1'} - 1}{\rho} - \left\{ \frac{1}{2} \left(\frac{2^{R_1'+R_2'} - 2^{R_2'}}{\rho} \right)^2 - \frac{2^{R_1'+R_2'} - 1}{\rho} \left(\frac{2^{R_1'+R_2'} - 2^{R_2'}}{\rho} \right) \right\} \right. \\
& \left. + \left\{ \frac{1}{2} \left(\frac{2^{R_1'} - 1}{\rho} \right)^2 - \frac{2^{R_1'+R_2'} - 1}{\rho} \left(\frac{2^{R_1'} - 1}{\rho} \right) \right\} \right] \\
& + \Phi_2(\beta_1, R_1' + R_2', R_2') \Phi_1(\beta_2, R_2') - \Phi_1(\beta_\mathrm{r}, 2R') \\
& \times \frac{1}{\beta_1\beta_2} \left(\frac{2^{R_1'+R'} - 1}{\rho} \frac{2^{2R'} - 2^{R_1'+R'}}{\rho} + \frac{2^{R_1'+R_2'} - 2^{R_2'}}{\rho} \frac{2^{R_2'} - 1}{\rho} \right) \\
& - \Phi_1(\beta_2, 2R') \frac{1}{\beta_1} \left(\frac{2^{2R'} - 2^{R_2'+R'}}{\rho} - \frac{2^{R_1'+R'} - 1}{\rho} \right) \\
& - \Phi_1(\beta_\mathrm{r}, 2R') \frac{1}{\beta_1\beta_2} \left[\left\{ -\frac{1}{2} \left(\frac{2^{2R'} - 2^{R_2'+R'}}{\rho} \right)^2 + \frac{2^{2R'} - 1}{\rho} \left(\frac{2^{2R'} - 2^{R_1'+R'}}{\rho} \right) \right\} \right. \\
& \left. + \left\{ \frac{1}{2} \left(\frac{2^{R_1'+R'} - 1}{\rho} \right)^2 - \frac{2^{2R'} - 1}{\rho} \left(\frac{2^{R_1'+R'} - 1}{\rho} \right) \right\} - \frac{2^{R_2'} - 1}{\rho} \frac{2^{2R'} - 2^{R_2'+R'}}{\rho} \right] \\
& - \Phi_2(\beta_2, 2R', R_1' + R') \Phi_1(\beta_\mathrm{r}, R_1' + R') \frac{1}{\beta_1} \frac{2^{R_1'+R'} - 2^{R_1'}}{\rho} - \Phi_2(\beta_1, 2R', R_2' + R') \\
& \times \left\{ \Phi_1(\beta_2, R_2' + R') + \Phi_1(\beta_\mathrm{r}, R_2' + R') \times \frac{1}{\beta_2} \frac{2^{R_2'+R'} - 2^{R_2'}}{\rho} \right\} - \Phi_1(\beta_2, R_2') \Phi_2(\beta_1, R_1' + R_2', R_2').
\end{aligned} \tag{32}$$

$$\begin{aligned}
p_{o,\mathrm{I}} = {} & \Phi_1(\beta_\mathrm{r}, 2R') \frac{1}{\beta_1\beta_2} \left[\frac{2^{2R'} - 2^{R_1'+R'}}{\rho} \frac{2^{R_1'} - 1}{\rho} - \left\{ \frac{1}{2} \left(\frac{2^{R_1'+R_2'} - 2^{R_2'}}{\rho} \right)^2 - \frac{2^{R_1'+R_2'} - 1}{\rho} \left(\frac{2^{R_1'+R_2'} - 2^{R_2'}}{\rho} \right) \right\} \right. \\
& \left. + \left\{ \frac{1}{2} \left(\frac{2^{R_1'} - 1}{\rho} \right)^2 - \frac{2^{R_1'+R_2'} - 1}{\rho} \left(\frac{2^{R_1'} - 1}{\rho} \right) \right\} \right] \\
& - \Phi_1(\beta_\mathrm{r}, 2R') \frac{1}{\beta_1\beta_2} \left(\frac{2^{R_1'+R'} - 1}{\rho} \frac{2^{2R'} - 2^{R_1'+R'}}{\rho} + \frac{2^{R_1'+R_2'} - 2^{R_2'}}{\rho} \times \frac{2^{R_2'} - 1}{\rho} \right) \\
& - \Phi_1(\beta_2, 2R') \frac{1}{\beta_1} \left(\frac{2^{2R'} - 2^{R_2'+R'}}{\rho} - \frac{2^{R_1'+R'} - 1}{\rho} \right) \\
& - \Phi_1(\beta_\mathrm{r}, 2R') \frac{1}{\beta_1\beta_2} \left[\left\{ \frac{2^{2R'} - 1}{\rho} \left(\frac{2^{2R'} - 2^{R_1'+R'}}{\rho} \right) - \frac{1}{2} \left(\frac{2^{2R'} - 2^{R_2'+R'}}{\rho} \right)^2 \right\} \right. \\
& \left. + \left\{ \frac{1}{2} \left(\frac{2^{R_1'+R'} - 1}{\rho} \right)^2 - \frac{2^{2R'} - 1}{\rho} \left(\frac{2^{R_1'+R'} - 1}{\rho} \right) \right\} - \frac{2^{R_2'} - 1}{\rho} \frac{2^{2R'} - 2^{R_2'+R'}}{\rho} \right] \\
& - \Phi_2(\beta_2, 2R', R_1' + R') \Phi_1(\beta_\mathrm{r}, R_1' + R') \frac{1}{\beta_1} \frac{2^{R_1'+R'} - 2^{R_1'}}{\rho} - \Phi_2(\beta_1, 2R', R_2' + R') \\
& \times \left\{ \Phi_1(\beta_2, R_2' + R') + \Phi_1(\beta_\mathrm{r}, R_2' + R') \frac{1}{\beta_2} \frac{2^{R_2'+R'} - 2^{R_2'}}{\rho} \right\}
\end{aligned} \tag{33}$$

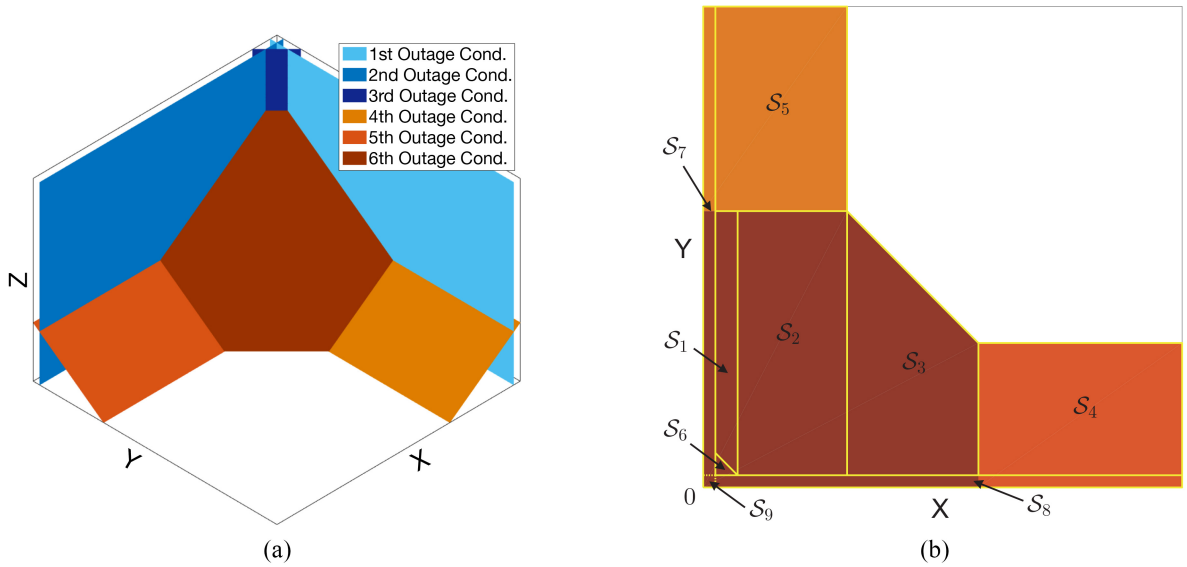

Fig. 10. Total outage region of the RN with inter-RN interference in the proposed uplink cooperative NOMA scheme. (a) In 3-D space. (b) On 2-D space (x–y axis).

TABLE II
INTEGRAL RANGES OF THE OUTAGE REGION OF THE RN WITH INTER-RN INTERFERENCE

s	$x_{1,s}$	$x_{2,s}$	$y_{1,s}$	$y_{2,s}$	$z_{1,s}$	$z_{2,s}$
1	$\frac{2^{R'}-2^{R'_2}}{\rho}$	$\frac{2^{R'_1}-1}{\rho}$	$\frac{2^{2R'}-2^{R'_1+R'}}{\rho}$	$-g_1+\frac{2^{R'}-1}{\rho}$	$-g_1-g_2+\frac{2^{2R'}-1}{\rho}$	
2	$\frac{2^{R'+R'_1}-1}{\rho}$	$\frac{2^{R'}-2^{R'_2}}{\rho}$	$\frac{2^{2R'}-2^{R'+R'_1}}{\rho}$	$\frac{2^{R'_2}-1}{\rho}$	$-g_1-g_2+\frac{2^{2R'}-1}{\rho}$	
3	$\frac{2^{2R'}-2^{R'+R'_2}}{\rho}$	$\frac{2^{R'+R'_1}-1}{\rho}$	$-g_1+\frac{2^{2R'}-1}{\rho}$	$\frac{2^{R'_2}-1}{\rho}$	$-g_1-g_2+\frac{2^{2R'}-1}{\rho}$	
4	∞	$\frac{2^{2R'}-2^{R'+R'_2}}{\rho}$	$\frac{2^{R'+R'_2}-1}{\rho}$	$\frac{2^{R'_2}-1}{\rho}$	$-g_2+\frac{2^{R'+R'_2}-1}{\rho}$	0
5	$\frac{2^{R'+R'_1}-1}{\rho}$	$\frac{2^{R'_1}-1}{\rho}$	∞	$\frac{2^{2R'}-2^{R'+R'_1}}{\rho}$	$-g_1+\frac{2^{R'+R'_1}-1}{\rho}$	
6	$\frac{2^{R'}-2^{R'_2}}{\rho}$	$\frac{2^{R'_1}-1}{\rho}$	$-g_1+\frac{2^{R'}-1}{\rho}$	$\frac{2^{R'_2}-1}{\rho}$	∞	
7	$\frac{2^{R'_2}-1}{\rho}$	0	∞	0	∞	
8	∞	0	$\frac{2^{R'_1}-1}{\rho}$	0	∞	
9	$\frac{2^{R'_1}-1}{\rho}$	0	$\frac{2^{R'_2}-1}{\rho}$	0	∞	

These conditions can be expressed as follows:

$$\begin{bmatrix}\pi_0\\ \pi_1\\ \vdots\\ \pi_K\\ \hline 1\end{bmatrix}=\left[\begin{array}{cccc}P_{0,0} & P_{1,0} & \cdots & P_{K,0}\\ \vdots & \vdots & \ddots & \vdots\\ P_{0,K-1} & P_{1,K-1} & \cdots & P_{K,K-1}\\ \hline P_{0,K} & 0 & \ldots & 0\\ 1 & 1 & \ldots & 1\end{array}\right]\begin{bmatrix}\pi_0\\ \pi_1\\ \vdots\\ \pi_K\end{bmatrix}. \quad (35)$$

By subtracting the vector $[\boldsymbol{\pi}^T \mid 0]^T$ from both sides, the following equation is obtained:

$$\begin{bmatrix}0\\ \vdots\\ 0\\ \hline 1\end{bmatrix}=\underbrace{\left[\begin{array}{ccc}\multicolumn{3}{c}{\mathbf{P}_K-\mathbf{I}_K}\\ \hline 1 & 1 & \ldots\ 1\end{array}\right]}_{\triangleq\mathbf{Q}_K}\begin{bmatrix}\pi_0\\ \pi_1\\ \vdots\\ \pi_K\end{bmatrix}. \quad (36)$$

Then, the pseudo-inverse matrix of the nonsquare matrix $\mathbf{Q}_K \in \mathbb{C}^{(K+2)\times(K+1)}$, $\mathbf{Q}_K^{\dagger} \in \mathbb{C}^{(K+1)\times(K+2)}$, contains the solution of the stationary distribution, as in the last column

$$\begin{bmatrix}\pi_0\\ \pi_1\\ \vdots\\ \pi_K\end{bmatrix}=\mathbf{Q}_K^{\dagger}\begin{bmatrix}0\\ \vdots\\ 0\\ \hline 1\end{bmatrix}=\left(\text{the last column of } \mathbf{Q}_K^{\dagger}\right). \quad (37)$$

Finally, we can attain (17).

APPENDIX C
PROOF OF THEOREM 3

The basic idea of the upper bound analysis for outage probability is to reduce the exact condition of successful JD in a complicated shape at the RN with inter-RN interference into a *cube-shaped* successful condition. In the coordinate system illustrated in Fig. 10, the edges of the cube are parallel to the axes (x-axis, y-axis, and z-axis) and extended to infinity in positive directions. Then, the cube does not intersect with the exact outage region, and the resultant probability becomes the

upper bound of the exact outage probability. The successful decoding condition with a cube-shaped region, $\bar{\mathscr{O}}_{\mathsf{r},2}^{\text{Prop.}}$, is given by

$$\bar{\mathscr{O}}_{\mathsf{r},2}^{\text{Prop.}} = \left\{ \begin{array}{l} \frac{N-1}{N}\log(1+\rho g_{1k}) > \bar{R}_1 \bigcap \\ \frac{N-1}{N}\log(1+\rho g_{2k}) > \bar{R}_2 \bigcap \\ \frac{N-1}{N}\log\left(1+\rho g_{1,k^*k}\right) > \bar{R}_{\mathsf{r}} \end{array} \right\} \tag{38}$$

where $\bar{R}_1$, $\bar{R}_2$, and $\bar{R}_{\mathsf{r}}$ denote the appropriate constants that satisfy the condition that $\bar{\mathscr{O}}_{\mathsf{r},2}^{\text{Prop.}} \subseteq \mathscr{O}_{\mathsf{r},2}^{\text{Prop.}}$ (this is equivalent to satisfying the upper-bounded outage condition). For convenience, let $Q_w \triangleq (2^{\bar{R}_w N/(N-1)} - 1)$ $(w \in \{1, 2, \mathsf{r}\})$. Then, for a given Q_1, Q_2, and Q_{r}, the upper bound of the outage probability using (38) is given by

$$\bar{p}_{o,\mathrm{I}} = 1 - e^{-\frac{1}{\rho}\left(\frac{1}{\beta_1}Q_1 + \frac{1}{\beta_2}Q_2 + \frac{1}{\beta_{\mathsf{r}}}Q_{\mathsf{r}}\right)}. \tag{39}$$

Next, the variables Q_1, Q_2, and Q_{r} must be carefully adjusted to make the upper-bound as tight as possible. In other words, (39) is minimized under the upper bound condition of the outage probability using the following linear programming:

$$\begin{aligned} \min_{Q_1,Q_2,Q_{\mathsf{r}}} \quad & \frac{1}{\beta_1}Q_1 + \frac{1}{\beta_2}Q_2 + \frac{1}{\beta_{\mathsf{r}}}Q_{\mathsf{r}} \\ \text{s.t.} \quad & \log\left(1 + \sum_{w\in\mathcal{W}} Q_w\right) \geq \frac{N\sum_{w\in\mathcal{W}} R_w}{N-1} \quad \forall \mathcal{W} \subseteq \{1,2,\mathsf{r}\} \\ & \qquad\qquad\qquad\qquad\qquad\qquad \text{and } \mathcal{W} \neq \{\mathsf{r}\} \\ & Q_{\mathsf{r}} \geq 0. \end{aligned} \tag{40}$$

In (40), the constraints are reexpressed as follows:

$$\begin{bmatrix} 1 & 0 & 0 \\ 0 & 1 & 0 \\ 1 & 1 & 0 \\ 1 & 0 & 1 \\ 0 & 1 & 1 \\ 1 & 1 & 1 \\ 0 & 0 & 1 \end{bmatrix} \begin{bmatrix} Q_1 \\ Q_2 \\ Q_{\mathsf{r}} \end{bmatrix} \geq \begin{bmatrix} 2^{R_1'} - 1 \\ 2^{R_2'} - 1 \\ 2^{R'} - 1 \\ 2^{R_1'+R'} - 1 \\ 2^{R_2'+R'} - 1 \\ 2^{2R'} - 1 \\ 0 \end{bmatrix}. \tag{41}$$

The solutions to the minimization problem are easily obtained according to β_1, β_2, and β_{r}, as listed in Table I. In Table I, subscripts m and M $(m, M \in \{1, 2\}, m \neq M)$ denote the index of ID with longer and shorter distances between IDs and the transmitting RN, respectively. This approach can also be applied to obtain the upper bound of the outage probability at an RN without inter-RN interference.

APPENDIX D
PROOF OF THEOREM 4

In order to analyze the diversity order of the proposed uplink cooperative NOMA technique, we obtain the dominant term in the outage probability expression for a high SNR regime. Applying the Taylor series expansion to (17), the outage probability is given by

$$\begin{aligned} \Pr\{\mathcal{O}\} &= \sum_{u=0}^{K}\left[1 - e^{-\frac{2^{\frac{N(R_1+R_2)}{N-1}}-1}{\beta_{\mathsf{ra}}\rho}}\sum_{m=0}^{M-1}\left(\frac{2^{\frac{N(R_1+R_2)}{N-1}}-1}{\beta_{\mathsf{ra}}\rho}\right)^m\frac{1}{m!}\right]^u\pi_u \\ &\overset{(a)}{=} \sum_{u=0}^{K}\left[1 - \left(\sum_{a=0}^{\infty}\frac{(-\zeta)^a}{a!}\rho^{-a}\right)\left(\sum_{m=0}^{M-1}\frac{\zeta^m}{m!}\rho^{-m}\right)\right]^u\pi_u \\ &= \sum_{u=0}^{K}\left[1 - \sum_{a=0}^{\infty}\sum_{m=0}^{M-1}(-1)^a\frac{\zeta^{a+m}}{a!m!}\rho^{-(a+m)}\right]^u\pi_u \end{aligned} \tag{42}$$

where $\zeta = (2^{N(R_1+R_2)/(N-1)} - 1)/\beta_{\mathsf{ra}}$, and (a) is derived by $e^{ax} = \sum_{n=0}^{\infty}[(ax)^n/n!]$. We can approximate (42) as follows:

$$\begin{aligned} \Pr\{\mathcal{O}\} &= \sum_{u=0}^{K}\left[1 - \sum_{a=0}^{\infty}\sum_{m=0}^{M-1}(-1)^a\frac{\zeta^{a+m}}{a!m!}\rho^{-(a+m)}\right]^u\pi_u \\ &= \sum_{u=0}^{K}\left[\sum_{a=1}^{\infty}\sum_{m=\max(0,M-a)}^{M-1}(-1)^{a+1}\frac{\zeta^{a+m}}{a!m!}\rho^{-(a+m)}\right]^u\pi_u \\ &\lesssim \sum_{u=0}^{K}\left(\frac{\zeta^M}{M!}\rho^{-M}\right)^u\pi_u. \end{aligned} \tag{43}$$

Next, we obtain the dominant term in the transition distribution matrix π_u in the high SNR regime. The transition distribution matrix in (37) is not expressed in closed-form. Thus, we use the upper-bounded outage probability at RNs (19) and observe the behavior of the dominant term in each element of the transition matrix in the stationary state. The upper bound of the outage probability at RNs with inter-RN interference is asymptotically approximated as follows:

$$\begin{aligned} \bar{p}_{o,\mathrm{I}} &= 1 - \exp\left(-\frac{1}{\rho}\left(\frac{1}{\beta_1}Q_1 + \frac{1}{\beta_2}Q_2 + \frac{1}{\beta_{\mathsf{r}}}Q_{\mathsf{r}}\right)\right) \\ &= 1 - \sum_{s=0}^{\infty}\frac{(-Q_{\mathrm{I}})^s}{s!}\rho^{-s} \approx Q_{\mathrm{I}}\rho^{-1} \end{aligned} \tag{44}$$

where $Q_I = (1/\beta_1)Q_1 + (1/\beta_2)Q_2 + (1/\beta_{\mathsf{r}})Q_{\mathsf{r}}$. As described in Appendix C, we can similarly obtain the upper-bounded outage probability at the RN without inter-RN interference, which is approximated in the high SNR regime as follows:

$$p_o \leq \bar{p}_o = 1 - \exp\left(-\frac{1}{\rho}\left(\frac{1}{\beta_1}Q_1 + \frac{1}{\beta_2}Q_2\right)\right) \approx Q\rho^{-1} \tag{45}$$

where $Q = (1/\beta_1)Q_1 + (1/\beta_2)Q_2$. By substituting (44) and (45) into (30) instead of $p_{o,\mathrm{I}}$ and p_o, respectively, the transition probability $P_{i,j}$ $(i, j \in \{0, 1, \ldots, K\})$ can be approximated as follows:

$$P_{i,j} \lesssim \begin{cases} \underbrace{\binom{K}{j}Q^{K-j}}_{\triangleq\, c_{0,j}}\rho^{-(K-j)}, & \text{if } i = 0 \\ \underbrace{\sum_{x=0}^{\min(i,j)}\binom{i-1}{x}\binom{K-i}{j-x}Q^{i-1-x}Q_{\mathrm{I}}^{K-i-j+x}}_{\triangleq\, c_{i,j}}\rho^{-(K-j-1)}, & \text{if } i \neq 0. \end{cases} \tag{46}$$

Hence, the transition matrix based on the upper bound of the outage probability is approximated in the high SNR regime as

follows:

$$\mathbf{P}_K \lesssim \begin{bmatrix} c_{0,0}\rho^{-K} & c_{1,0}\rho^{2-K} & \cdots & c_{K,0}\rho^{2-K} \\ c_{0,1}\rho^{1-K} & c_{1,1}\rho^{3-K} & \cdots & c_{K,1}\rho^{3-K} \\ \vdots & \vdots & \ddots & \vdots \\ c_{0,K-1}\rho^{-1} & c_{1,K-1}\rho^{0} & \cdots & c_{K,K-1}\rho^{0} \\ c_{0,K}\rho^{0} & 0 & \cdots & 0 \end{bmatrix}. \quad (47)$$

According to the ergodic theorem, $\lim_{n\to\infty}(\mathbf{P}_K^n)_{i+1,j+1} = \pi_j$ where $(\mathbf{A})_{r,c}$ denotes the (r,c)th element of matrix $\mathbf{A}$, and the approximated $\mathbf{P}_K^{n+1}$ $(n>1)$ provides meaningful insights

$$\mathbf{P}_K^{n+1} \lesssim \begin{bmatrix} c_{0,K}c_{K,0}^n\rho^{1-K} & c_{1,K-1}c_{K-1,0}^n\rho^{1-K} & \cdots & c_{K,K-1}c_{K-1,0}^n\rho^{1-K} \\ c_{0,K}c_{K,1}^n\rho^{2-K} & c_{1,K-1}c_{K-1,1}^n\rho^{2-K} & \cdots & c_{K,K-1}c_{K-1,0}^n\rho^{2-K} \\ \vdots & \vdots & \ddots & \vdots \\ c_{0,K}c_{K,K-1}^n\rho^{0} & c_{1,K-1}c_{K-1,K-1}^n\rho^{0} & \cdots & c_{K,K-1}c_{K-1,0}^n\rho^{0} \\ c_{0,K}c_{K,K}^n\rho^{1-K} & c_{1,K-1}c_{K-1,K}^n\rho^{1-K} & \cdots & c_{K,K-1}c_{K-1,0}^n\rho^{1-K} \end{bmatrix} \quad (48)$$

where $c_{i,j}^n$ denotes the coefficient for ρ at the $(i+1,j+1)$th element in $\mathbf{P}_K^n$. The transition probability from any state to state $j \in \{0,1,\ldots,K\}$ is proportional to $\rho^{-(K-j-1)}$ when $j \neq K$ and $\rho^{-(K-1)}$ when $j=K$

$$-\lim_{\rho\to\infty}\frac{\log\pi_j}{\log\rho} = \begin{cases} K-j-1, & \text{if } j\neq K \\ K-1, & \text{if } j=K. \end{cases} \quad (49)$$

Moreover, by considering a dominant transition path and some value of $c_{i,j}$, i.e., $c_{K-1,K-1} = c_{0,K} = 1$, we obtain a closed formed and approximated transition distribution as

$$\boldsymbol{\pi} \lesssim \begin{bmatrix} c_{K-1,0}\rho^{1-K} \\ c_{K-1,1}\rho^{2-K} \\ \vdots \\ c_{K-1,K-2}\rho^{-1} \\ 1 \\ c_{K-1,0}\rho^{1-K} \end{bmatrix} \in \mathbb{R}^{K+1}. \quad (50)$$

Finally, by substituting (50) into (43), we verify that the diversity order of the proposed uplink cooperative NOMA scheme is equal to $K-1$

$$-\lim_{\rho\to\infty}\frac{\log\left[\sum_{u=0}^{K}\left(\frac{\zeta^M}{M!}\rho^{-M}\right)^u\pi_u\right]}{\log\rho} \overset{(a)}{=} K-1 \quad (51)$$

where (a) is derived from the fact that when $u=0$, the summation has an order of only $K-1$, which is the smallest order for $1/\rho$ when $M\geq 2$.

REFERENCES

[1] G. A. Akpakwu, B. J. Silva, G. P. Hancke, and A. M. Abu-Mahfouz, "A survey on 5G networks for the Internet of Things: Communication technologies and challenges," *IEEE Access*, vol. 6, pp. 3619–3647, Dec. 2017.

[2] X. Chen, D. W. K. Ng, W. Yu, E. G. Larsson, N. Al-Dhahir, and R. Schober, "Massive access for 5G and beyond," *IEEE J. Sel. Areas Commun.*, vol. 39, no. 3, pp. 615–637, Mar. 2021.

[3] Z. Zhang *et al.*, "6G wireless networks: Vision, requirements, architecture, and key technologies," *IEEE Veh. Technol. Mag.*, vol. 14, no. 3, pp. 28–41, Sep. 2019.

[4] D.-T. Phan-Huy *et al.*, "Single-carrier spatial modulation for the Internet of Things: Design and performance evaluation by using real compact and reconfigurable antennas," *IEEE Access*, vol. 7, pp. 18978–18993, Jan. 2019.

[5] M. Jia, Z. Yin, Q. Guo, G. Liu, and X. Gu, "Downlink design for spectrum efficient IoT network," *IEEE Internet Things J.*, vol. 5, no. 5, pp. 3397–3404, Oct. 2018.

[6] X. Liu, M. Jia, X. Zhang, and W. Lu, "A novel multichannel Internet of Things based on dynamic spectrum sharing in 5G communication," *IEEE Internet Things J.*, vol. 6, no. 4, pp. 5962–5970, Aug. 2019.

[7] S. Aslam, W. Ejaz, and M. Ibnkahla, "Energy and spectral efficient cognitive radio sensor networks for Internet of Things," *IEEE Internet Things J.*, vol. 5, no. 4, pp. 3220–3233, Aug. 2018.

[8] Q. Wu, W. Chen, D. W. K. Ng, and R. Schober, "Spectral and energy-efficient wireless powered IoT networks: NOMA or TDMA?" *IEEE Trans. Veh. Technol.*, vol. 67, no. 7, pp. 6663–6667, Jul. 2018.

[9] Z. Ding *et al.*, "Application of non-orthogonal multiple access in LTE and 5G networks," *IEEE Commun. Mag.*, vol. 55, no. 2, pp. 185–191, Feb. 2017.

[10] Y. Saito, Y. Kishiyama, A. Benjebbour, T. Nakamura, A. Li, and K. Higuchi, "Non-orthogonal multiple access (NOMA) for cellular future radio access," in *Proc. IEEE Veh. Technol. Conf. (VTC)*, Jun. 2013, pp. 1–5.

[11] B. Makki, K. Chitti, A. Behravan, and M.-S. Alouini, "A survey of NOMA: Current status and open research challenges," *IEEE Open J. Commun. Soc.*, vol. 1, pp. 179–189, Jan. 2020.

[12] T. Lv, Z. Lin, P. Huang, and J. Zeng, "Optimization of the energy-efficient relay-based massive IoT network," *IEEE Internet Things J.*, vol. 5, no. 4, pp. 3043–3058, Aug. 2018.

[13] J. Men, J. Ge, and C. Zhang, "Performance analysis for Downlink relaying aided non-orthogonal multiple access networks with imperfect CSI over Nakagami-*m* fading," *IEEE Access*, vol. 5, pp. 998–1004, Nov. 2016.

[14] X. Liang, Y. Wu, D. W. K. Ng, Y. Zuo, S. Jin, and H. Zhu, "Outage performance for cooperative NOMA transmission with an AF relay," *IEEE Commun. Lett.*, vol. 21, no. 11, pp. 2428–2431, Nov. 2017.

[15] M. F. Kader and S. Y. Shin, "Coordinated direct and relay transmission using uplink NOMA," *IEEE Wireless Commun. Lett.*, vol. 7, no. 3, pp. 400–403, Jun. 2018.

[16] Y. Liu *et al.*, "Performance analysis of a Downlink cooperative NOMA network over Nakagami- *m* fading channels," *IEEE Access*, vol. 6, pp. 53034–53043, Sep. 2018.

[17] H. Liu, Z. Ding, K. J. Kim, K. S. Kwak, and H. V. Poor, "Decode-and-forward relaying for cooperative NOMA systems with direct links," *IEEE Trans. Wireless Commun.*, vol. 17, no. 12, pp. 8077–8093, Dec. 2018.

[18] H. Liu, N. I. Miridakis, T. A. Tsiftsis, K. J. Kim, and K. S. Kwak, "Coordinated uplink transmission for cooperative NOMA systems," in *Proc. IEEE Global Commun. Conf. (GLOBECOM)*, Dec. 2018, pp. 1–6.

[19] Z. Mobini, M. Mohammadi, B. K. Chalise, H. A. Suraweera, and Z. Ding, "Beamforming design and performance analysis of full-duplex cooperative NOMA systems," *IEEE Trans. Wireless Commun.*, vol. 18, no. 6, pp. 3295–3311, Jun. 2019.

[20] P. Xu, J. Quan, Z. Yang, G. Chen, and Z. Ding, "Performance analysis of buffer-aided hybrid NOMA/OMA in cooperative uplink system," *IEEE Access*, vol. 7, pp. 168759–168773, Nov. 2019.

[21] X. Li, M. Liu, C. Deng, P. T. Mathiopoulos, Z. Ding, and Y. Liu, "Full-duplex cooperative NOMA relaying systems with I/Q imbalance and imperfect SIC," *IEEE Wireless Commun. Lett.*, vol. 9, no. 1, pp. 17–20, Jan. 2020.

[22] D. Korpi, L. Anttila, V. Syrjala, and M. Valkama, "Widely linear digital self-interference cancellation in direct-conversion full-duplex transceiver," *IEEE J. Sel. Areas Commun.*, vol. 32, no. 9, pp. 1674–1687, Sep. 2014.

[23] Y. Alsaba, C. Y. Leow, and S. K. A. Rahim, "Full-duplex cooperative non-orthogonal multiple access with beamforming and energy harvesting," *IEEE Access*, vol. 6, pp. 19726–19738, 2018.

[24] L. Lei, E. Lagunas, S. Chatzinotas, and B. Ottersten, "NOMA aided interference management for full-duplex self-backhauling HetNets," *IEEE Commun. Lett.*, vol. 22, no. 8, pp. 1696–1699, Aug. 2018.

[25] Y. Wu, L. P. Qian, H. Mao, X. Yang, H. Zhou, and X. Shen, "Optimal power allocation and scheduling for non-orthogonal multiple access relay-assisted networks," *IEEE Trans. Mobile Comput.*, vol. 17, no. 11, pp. 2591–2606, Nov. 2018.

[26] A. Tregancini, E. E. B. Olivo, D. P. M. Osorio, C. H. M. de Lima, and H. Alves, "Performance analysis of full-duplex relay-aided NOMA systems using partial relay selection," *IEEE Trans. Veh. Technol.*, vol. 69, no. 1, pp. 622–635, Jan. 2020.
[27] Z. Yu, C. Zhai, J. Liu, and H. Xu, "Cooperative relaying based non-orthogonal multiple access (NOMA) with relay selection," *IEEE Trans. Veh. Technol.*, vol. 67, no. 12, pp. 11606–11618, Dec. 2018.
[28] Z. Ding, H. Dai, and H. V. Poor, "Relay selection for cooperative NOMA," *IEEE Wireless Commun. Lett.*, vol. 5, no. 4, pp. 416–419, Aug. 2016.
[29] Z. Yang, Z. Ding, Y. Wu, and P. Fan, "Novel relay selection strategies for cooperative NOMA," *IEEE Trans. Veh. Technol.*, vol. 66, no. 11, pp. 10114–10123, Nov. 2017.
[30] P. Xu, Z. Yang, Z. Ding, and Z. Zhang, "Optimal relay selection schemes for cooperative NOMA," *IEEE Trans. Veh. Technol.*, vol. 67, no. 8, pp. 7851–7855, Aug. 2018.
[31] X. Yue, Y. Liu, S. Kang, A. Nallanathan, and Z. Ding, "Spatially random relay selection for full/half-duplex cooperative NOMA networks," *IEEE Trans. Commun.*, vol. 66, no. 8, pp. 3294–3308, Aug. 2018.
[32] Y. Kim, K. Yamazaki, and B. C. Jung, "Adaptive successive transmission in virtual full-duplex cooperative NOMA," in *Proc. IEEE Wireless Commun. Netw. Conf. (WCNC)*, Apr. 2018, pp. 1–6.
[33] Y. Kim, K. Yamazaki, and B. C. Jung, "Virtual full-duplex cooperative NOMA: Relay selection and interference cancellation," *IEEE Trans. Wireless Commun.*, vol. 18, no. 12, pp. 5882–5893, Dec. 2019.
[34] M. Elbayoumi, M. Kamel, W. Hamouda, and A. Youssef, "NOMA-assisted machine-type communications in UDN: State-of-the-art and challenges," *IEEE Commun. Surveys Tuts.*, vol. 22, no. 2, pp. 1276–1304, 2nd Quart., 2020.
[35] T. M. Cover and J. A. Thomas, *Elements of Information Theory*, 2nd ed. New Jersey, NJ, USA: Wiley, 2006.
[36] J. S. Yeom, H. S. Jang, K. S. Ko, and B. C. Jung, "BER performance of uplink NOMA with joint maximum-likelihood detector," *IEEE Trans. Veh. Technol.*, vol. 68, no. 10, pp. 10295–10300, Oct. 2019.
[37] Y. Zhang, K. Peng, Z. Chen, and J. Song, "SIC vs. JD: Uplink NOMA techniques for M2M random access," in *Proc. IEEE Int. Conf. Commun. (ICC)*, May 2017, pp. 1–6.
[38] S. A. Tegos, P. D. Diamantoulakis, A. S. Lioumpas, P. G. Sarigiannidis, and G. K. Karagiannidis, "Slotted ALOHA with NOMA for the next generation IoT," *IEEE Trans. Commun.*, vol. 68, no. 10, pp. 6289–6301, Oct. 2020.
[39] S. A. Tegos, P. D. Diamantoulakis, J. Xia, L. Fan, and G. K. Karagiannidis, "Outage performance of uplink NOMA in land mobile satellite communications," *IEEE Wireless Commun. Lett.*, vol. 9, no. 10, pp. 1710–1714, Oct. 2020.
[40] S. Timotheou and I. Krikidis, "Fairness for non-orthogonal multiple access in 5G systems," *IEEE Signal Process. Lett.*, vol. 22, no. 10, pp. 1647–1651, Oct. 2015.
[41] D. Zhai and R. Zhang, "Joint admission control and resource allocation for multi-carrier uplink NOMA networks," *IEEE Wireless Commun. Lett.*, vol. 7, no. 6, pp. 922–925, Dec. 2018.
[42] W. Ahsan, W. Yi, Z. Qin, Y. Liu, and A. Nallanathan, "Resource allocation in uplink NOMA-IoT networks: A reinforcement-learning approach," *IEEE Trans. Wireless Commun.*, vol. 20, no. 8, pp. 5083–5098, Aug. 2021.
[43] M. Wu, Y. Xiao, Y. Gao, and M. Xiao, "Dynamic socially-motivated D2D relay selection with uniform QoE criterion for multi-demands," *IEEE Trans. Commun.*, vol. 68, no. 6, pp. 3355–3368, Jun. 2020.
[44] R. Rajashekar, K. V. S. Hari, and L. Hanzo, "Antenna selection in spatial modulation systems," *IEEE Commun. Lett.*, vol. 17, no. 3, pp. 521–524, Mar. 2013.
[45] M. Wen, X. Cheng, M. Ma, B. Jiao, and H. V. Poor, "On the achievable rate of OFDM with index modulation," *IEEE Trans. Signal Process.*, vol. 64, no. 8, pp. 1919–1932, Apr. 2016.
[46] D. Tse and P. Viswanath, *Fundamentals of Wireless Communication*. Cambridge, U.K.: Cambridge Univ. Press, 2005.
[47] "Minimum requirements related to technical performance for IMT-2020 radio interface(s)," Int. Telecommun. Union, Geneva, Switzerland, Rep. ITU-R M.2410–0, Nov. 2017.

Jeong Seon Yeom (Student Member, IEEE) received the B.S. degree in electronics engineering and the M.S. degree in electronics, radio sciences, and engineering and information communications engineering from Chungnam National University, Daejeon, South Korea, in 2017 and 2019, respectively, where he is currently pursuing the Ph.D. degree in communications and signal processing in electronics engineering.

His research interests include nonorthogonal multiple access, cooperative relaying systems, stochastic geometry, and reconfigurable intelligent surface.

Young-Bin Kim (Member, IEEE) received the B.Sc. degree in electrical communications engineering in 2008 and the M.Sc. and Ph.D. degrees in electrical engineering from the Korea Advanced Institute of Science and Technology (KAIST), Daejeon, South Korea, in 2010 and 2017, respectively.

He was a Postdoctoral Research Scholar with KAIST from March 2017 to April 2017. He was an Associate Research Engineer with KDDI Research, Inc., Saitama, Japan, from May 2017 to May 2019 and a Section Manager of Rakuten Mobile, Inc., Tokyo, Japan, from May 2019 to December 2021. He is currently a Field Application Engineer with VIAVI Solutions, Inc., Tokyo.

Dr. Kim received the Korean Institute of Communications and Information Sciences Outstanding Paper Award in 2016. He also received the IEICE 2018 Joint Conference on Satellite Communications Best Paper Award in 2018.

Bang Chul Jung (Senior Member, IEEE) received the B.S. degree in electronics engineering from Ajou University, Suwon, South Korea, in 2002, and the M.S. and Ph.D degrees in electrical and computer engineering from the Korea Advanced Institute of Science and Technology (KAIST), Daejeon, South Korea, in 2004 and 2008, respectively.

He was a Senior Researcher/Research Professor with the KAIST Institute for Information Technology Convergence, Daejeon, from January 2009 to February 2010. From March 2010 to August 2015, he was a faculty of Gyeongsang National University, Tongyeong, South Korea. He is currently a Professor with the Department of EE, Chungnam National University, Daejeon. His research interests include 6G wireless communications, wireless IoT communications, statistical signal processing, information theory, wireless localization, interference management, radar signal processing, spectrum sharing, multiple antennas, multiple access techniques, radio resource management, machine learning, and GNSS receiver signal processing.

Dr. Jung was the recipient the the 5th IEEE Communication Society Asia–Pacific Outstanding Young Researcher Award in 2011, the KICS Haedong Young Scholar Award in 2015, and the 29th Young Researcher Award in 2019. He has been serving as an Associate Editor of *IEEE Vehicular Technology Magazine* since May 2020. He has been serving as an Associate Editor of *IEICE Transactions on Fundamentals of Electronics, Communications, and Computer Sciences* since 2018.